(19) Europäisches Patentamt
European Patent Office
Office européen des brevets

(11) **EP 4 474 529 A2**

(12) **EUROPEAN PATENT APPLICATION**

(43) Date of publication:
11.12.2024 Bulletin 2024/50

(21) Application number: **24207009.2**

(22) Date of filing: **07.09.2018**

(51) International Patent Classification (IPC):
C25B 11/091 *(2021.01)*

(52) Cooperative Patent Classification (CPC):
C25B 3/25; C25B 3/07; C25B 3/26; C25B 11/052; C25B 11/089; C25B 11/091

(84) Designated Contracting States:
AL AT BE BG CH CY CZ DE DK EE ES FI FR GB GR HR HU IE IS IT LI LT LU LV MC MK MT NL NO PL PT RO RS SE SI SK SM TR

(30) Priority: **07.09.2017 US 201762555503 P**
22.03.2018 US 201862646816 P

(62) Document number(s) of the earlier application(s) in accordance with Art. 76 EPC:
18853747.6 / 3 679 177

(71) Applicant: **The Trustees of Princeton University**
Princeton, NJ 08544 (US)

(72) Inventors:
- **BOCARSLY, Andrew**
  Plainsboro, 08536 (US)
- **PARIS, Aubrey**
  Delran, 08075 (US)
- **FRANCIS, Sonja**
  Princeton, 08540 (US)
- **CHU, An**
  Amherst, 01002 (US)

(74) Representative: **Greenwoods**
Queens House
55-56 Lincoln's Inn Fields
London WC2A 3LJ (GB)

Remarks:
This application was filed on 16.10.2024 as a divisional application to the application mentioned under INID code 62.

(54) **BINARY ALLOYS AND OXIDES THEREOF FOR ELECTROCATALYTIC REDUCTION OF CARBON DIOXIDE**

(57) In one aspect, systems for providing oxygenated organic products are described. In some embodiments, a system comprises an electrochemical cell including an electrolyte solution comprising CO_2, and an electrode comprising an alloy and/or mixture of metal oxides. The electrode comprises an electrocatalytic site for reduction of CO_2 to CO, wherein CO is incorporated into the oxygenated organic products. In some embodiments, the alloy comprises at least one of a transition metal and post-transition metal. Moreover, metal oxides of the electrode can comprise at least one of a transition metal oxide and post-transition metal oxide.

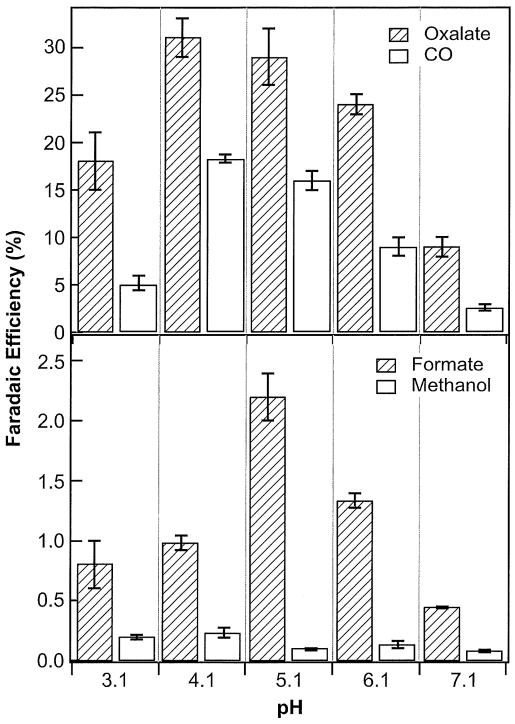

FIG. 7

EP 4 474 529 A2

Description

STATEMENT OF GOVERNMENT RIGHTS

[0001] This invention was made with government support under Grant No. CHE1308652 awarded by the National Science Foundation. The government has certain rights in the invention.

RELATED APPLICATION DATA

[0002] The present application claims priority to United States Provisional Patent Application Serial Number 62/555,503 filed September 7, 2017 and United States Provisional Patent Application Serial Number 62/464,816 filed March 22, 2018, each of which is incorporated herein by reference in its entirety.

FIELD

[0003] The present invention relates to the electrocatalytic reduction of CO_2 and, in particular, to the electrocatalytic reduction of CO_2 via binary alloy systems and/or oxides thereof.

BACKGROUND

[0004] Global atmospheric CO_2 concentrations have risen continuously for the past two centuries largely due to anthropogenic activities such as fossil fuel combustion, industrial manufacturing, and land clearing. This is cause for alarm because effects of high CO_2 levels include changes in water availability and food production capacity as well as implications for human health. The burning of fossil fuels not only sustains high CO_2 levels, but it also reduces our access to compounds which are critical chemical feedstocks. The electrochemical transformation of CO_2 into chemical feedstocks and energy sources offers a potential solution to this far-reaching problem, effectively turning a societal hindrance into practical products.

SUMMARY

[0005] Briefly, a system for providing oxygenated organic products comprises an electrochemical cell including an electrolyte solution comprising CO_2, and a working electrode comprising a transition metal/post transition metal (TM/PTM) binary alloy and/or oxide(s) thereof for electrocatalytic reduction of the CO_2 to the oxygenated organic products. In some embodiments, the oxygenated organic products comprise two or more carbon atoms and/or two or more oxygen atoms. Binary alloy of the working electrode can be of the formula TM_xPTM_y, wherein x and y are integers independently selected from 1 to 10. As described further herein, binary alloy of the working electrode may be in oxide form wherein one or both of the transition metal and post transition metal are metal oxides. Oxygenated organic products produced by the system can comprise one or more of propanol, butanol, ethanol, oxalate, formic acid or formate and acetone. In some embodiments, oxygenated organic products further include a single oxygen atom, including CO and methanol.

[0006] In another aspect, a system for providing oxygenated organic products comprises an electrochemical cell including an electrolyte solution comprising CO_2, and an electrode comprising an alloy and/or mixture of metal oxides. The electrode comprises an electrocatalytic site for reduction of CO_2 to CO, wherein CO is incorporated into the oxygenated organic products. In some embodiments, the alloy comprises at least one of a transition metal and post-transition metal. Moreover, metal oxides of the electrode can comprise at least one of a transition metal oxide and post-transition metal oxide.

[0007] In another aspect, a system for providing organic products comprises an electrochemical cell including an electrolyte solution comprising CO_2, and a working electrode comprising a transition metal/post-transition metal (TM/PTM) binary alloy and/or oxides thereof for electrocatalytic reduction of the CO_2 to the organic products. In some embodiments, binary alloy excludes nickel and gallium. Notably, binary metal oxides comprising nickel and gallium are not excluded. Organic products produced by the system can comprise one carbon atom, two carbon atoms, three carbon atoms or mixtures thereof. Additionally, the organic products can be oxygenated, in some embodiments.

[0008] In another aspect, methods of forming oxygenated organic products are described herein. In some embodiments, a method of forming oxygenated organic products includes providing an electrochemical cell including an electrolyte solution comprising CO_2, and a working electrode comprising a transition metal/post transition metal (TM/PTM) binary alloy and/or oxide(s) thereof and electrocatalytically reducing the CO_2 to the oxygenated organic products. The oxygenated organic products can comprise two or more carbon atoms and/or two or more oxygen atoms. Oxygenated products can include one or more of propanol, butanol, ethanol, oxalate, formic acid or formate and acetone. In some embodiments, oxygenated products additionally include a single oxygen atom including CO and methanol.

[0009] In another aspect, a method of forming oxygenated organic products comprises providing an electrochemical cell including an electrolyte solution comprising CO_2, and an electrode comprising an alloy and/or mixture of metal oxides. CO_2 is reduced to CO at an electrocatalytic site on the electrode, and the oxygenated organic products are derived from the CO. In some embodiments, for example, the oxygenated products comprise oxalate.

[0010] In another aspect, methods of forming organic products are described. In some embodiments, a method of forming organic products comprises providing an electrochemical cell including an electrolyte solution comprising CO_2, and a working electrode comprising a transition metal/post-transition metal (TM/PTM) binary alloy and/or oxide(s) thereof and electrocatalytically reducing the CO_2 to the organic products. In some embodiments, the binary alloy excludes combination of nickel and gallium, without excluding binary metal oxide composition including oxides of nickel and/or gallium. Organic products can comprise one carbon atom, two carbon atoms, three carbon atoms or mixtures thereof. Additionally, the organic products can be oxygenated, in some embodiments.

[0011] In a further aspect, methods of oxalate production are described. In some embodiments, a method of oxalate production comprises providing an electrochemical cell including an electrolyte solution comprising CO_2, and a working electrode comprising a transition metal oxide/post-transition metal oxide composite and electrocatalytically reducing the CO_2 to oxalate via generating CO and methanol from the CO_2. In some embodiments, CO is incorporated into the oxalate product, and methanol is excluded from the oxalate product. Moreover, oxalate can be produced at Faradaic efficiencies of at least 60 percent. As described further herein, various aspects and/or parameters of oxalate production methods can be altered or adjusted to achieve higher Faradaic efficiencies, including efficiencies greater than 70 percent or greater than 80 percent.

[0012] These and other embodiments are described in more detail in the following detailed description.

BRIEF DESCRIPTION OF THE DRAWINGS

[0013]

FIG. 1 provides powder X-ray diffraction of Ni_3Al film on glassy carbon referenced to PDF 01-071-5883. Scanning electron microscopy (SEM) images of the Ni_3Al film are also provided on the right side.

FIG. 2(A) are cyclic voltammograms obtained using Ni_3Al on glassy carbon under CO_2 (red) and Ar (black). Voltammograms were obtained at a scan rate of 100 mV/s with Pt mesh counter and Ag/AgCl reference electrodes in 0.1 M K_2SO_4 at pH 4.5.

FIG. 2(B) provides ^{1}H-NMR of 0.1 M K_2SO_4 electrolyte solution following bulk electrolysis at -1.38 V, indicating the presence of 1-propanol, methanol, and formate as major products. The broad peak at 4.66 ppm is a suppressed water signal, and all peaks are referenced to a 1,4-dioxane internal standard.

FIG. 2(C) provides ^{13}C-NMR confirming the presence of ethanol.

FIG. 2(D) provides ^{1}H-^{13}C HSQC indicating that ^{13}C-labelled acetone was produced.

FIG. 3(A) - Faradaic efficiencies for CO, 1-propanol, methanol, and formate are reported at a range of applied potentials.

FIG. 3(B) - Faradaic efficiencies for H_2, CO, and liquid products are plotted as a function of pH and confirm charge balance (top); the liquid product distribution is provided in the lower portion of panel (B).

FIG. 4 quantifies the major liquid products, 1-propanol and methanol, plotted versus the amount of charge passed using (A) CO_2 and (B) CO feedstocks.

FIG. 5A presents an XRD pattern (left) of Cr_2O_3-Ga_2O_3 referenced to Cr_2O_3 (PDF 00-038-1479) and Ga_2O_3 (PDF 01-074-1610); and an SEM image (right) of Cr_2O_3-Ga_2O_3 platelets.

FIG. 5B is a fitted XPS spectra of Cr (left) and Ga (right), indicating that the surface is primarily made up of metal oxides. Peaks were referenced to adventitious carbon at 284.5 eV (not shown).

FIG. 6 is an IR spectrum of calcium oxalate derived from Cr_2O_3-Ga_2O_3 mediated electrolysis, confirming that oxalate is a CO_2 reduction product.

FIG. 7 illustrates pH dependence of Faradaic efficiencies for carbon-containing products. Experiments were performed at -1.38 V vs. Ag/AgCl using CO_2-saturated 0.1 M KCl buffered with $KHCO_3$ (pH > 4) or adjusted with HCl (pH < 4).

FIG. 8 illustrates potential dependence of Faradaic efficiencies for carbon-containing products. Experiments used pH 4.05, 0.1 M KCl electrolyte, and all potentials tested were more positive than the thermodynamic potential for one-electron reduction of CO_2. Optimal oxalate production was achieved at -1.48 V vs. Ag/AgCl.

FIG. 9 illustrates Faradaic efficiencies of carbon-containing products. While oxalate generation is suppressed at high KCl concentrations, low CO and high formate Faradaic efficiencies contribute to decreased oxalate production at low KCl concentrations. Electrolyses were performed at -1.48 V vs. Ag/AgCl.

FIG. 10 illustrates Faradaic efficiencies of carbon-containing products. Cr-rich stoichiometries result in the lowest efficiencies for CO. Electrolyses were performed at -1.48 V vs. Ag/AgCl in 0.1 M KCl (pH 4.1).

DETAILED DESCRIPTION

[0014] Embodiments described herein can be understood more readily by reference to the following detailed description and examples and their previous and following descriptions. Elements, apparatus and methods described herein, however, are not limited to the specific embodiments presented in the detailed description and examples. It should be recognized that these embodiments are merely illustrative of the principles of the present invention. Numerous modifications and adaptations will be readily apparent to those of skill in the art without departing from the scope of the invention.

[0015] In one aspect, systems employing binary alloys and/or oxide(s) thereof for the electrocatalytic reduction of CO_2 to various organic products are described. Binary alloys and/or oxides thereof suitable for electrocatalytic reduction of CO_2 comprise a transition metal and a post-transition metal (TM/PTM). In some embodiments, the transition metal is a first row transition metal. Moreover, post-transition metals can be selected from Groups IIB-VA of the Periodic Table. Groups of the Periodic Table referenced herein are identified according to the CAS designation. Binary alloys, in some embodiments are of the formula TM_xPTM_y, wherein x and y are integers independently selected from 1 to 10. Transition metal and post-transition metal can be combined in any ratio operable for the electrocatalytic reduction of CO_2 into various organic products. In some embodiments, for example, x is 3 and y is 1. In other embodiments, x can range from 1 to 9 and y can range from 1 to 6. Table I provides a listing of various binary alloys operable for the electrocatalytic reduction of CO_2 into various organic products, including oxygenated products comprising two or more carbon atoms and/or two or more oxygen atoms.

Table I - TM_xPTM_y, wherein x = 3 and y =1

Ni-Al
Ni-Ga
Ni-In
Cu-Al
Fe-Ga
Fe-Al
Mn-Al
Mn-Ga
Co-Al
Ni-Zn
Co-Ga
Cr-Al
Cr-Ga
Ag-Al
Ag-Ga

As described herein, the binary alloy can be in oxide form. For example, at least one of the transition metal and post transition metal is a metal oxide. In some embodiments, both the transition metal and post transition metal are metal oxides. Binary alloy may be partially oxidized or fully oxidized. Binary metal oxides, for example, may form surface and/or bulk regions of the material administering the electrocatalytic reduction of CO_2. Any oxides of the binary alloy systems listed in Table I are contemplated. In some embodiments, for example, the working electrode comprises the binary system of chromium oxide and gallium oxide including, but not limited to, Cr_2O_3-Ga_2O_3. Moreover, stoichiometries or ratios of the transition metal and post-transition metal can remain the same in the metal oxide as in the binary alloy. Accordingly, the values provided for x and y above apply to metal oxide embodiments. In chromium oxide-gallium oxide embodiments, for example, the ratio of chromium to gallium can be 3:1.

[0016] In some embodiments, a binary alloy and/or oxides thereof contain one metal that can bind CO_2 at the electrode interface via a Lewis acid interaction and second metal that is moderately effective at participating in proton coupled electron transfers. In other embodiments, binary alloys and/or associated oxides of interest for electrocatalytic CO_2 reduction contain a d^9 valence electron count.

[0017] Binary alloy and/or oxides thereof can be provided as a thin film on the working electrode of the electrochemical

cell. The thin film of binary alloy and/or oxides thereof can be deposited on any substrate consistent with the objectives of the present invention. In some embodiments, for example, the thin film of alloy and/or oxide is deposited on glassy carbon.

[0018] The electrochemical cell also comprises an electrolyte solution having CO_2 dissolved therein. Any electrolyte solution consistent with the objectives of the present invention can be employed, including aqueous electrolyte solution. In some embodiments, aqueous electrolyte solution comprises alkali metal salt or alkaline earth metal salt. The electrolyte solution may also comprise CO in addition to CO_2, in some embodiments. The electrolyte solution can have neutral or acidic pH, in some embodiments. The electrolyte solution, for example, can have pH ranging from 3-7 or from 3-6.5. In other embodiments, pH of the electrolyte solution ranges from 4-6. Oxygenated organic products formed by the electrocatalytic reduction of CO_2 at the working electrode can include one or more of propanol, butanol, ethanol, oxalate, formic acid or formate and acetone. In some embodiments, oxygenated products include a single oxygen atom, such as CO and methanol.

[0019] TM/PTM binary alloy and/or oxides thereof of the working electrode are operable to form additional organic products from the electrocatalytic reduction of CO_2. These organic products can comprise one carbon atom, two carbon atoms, three carbon atoms or mixtures thereof. Such organic products can be aliphatic or oxygenated. In some embodiments, TM/PTM binary alloy excludes the combination of nickel and gallium for the production of aliphatic products and oxygenated products comprising a single carbon atom and/or single oxygen atom.

[0020] In another aspect, a system for providing oxygenated organic products comprises an electrochemical cell including an electrolyte solution comprising CO_2, and an electrode comprising an alloy and/or mixture of metal oxides. The electrode comprises an electrocatalytic site for reduction of CO_2 to CO, wherein CO is incorporated into the oxygenated organic products. In some embodiments, the alloy comprises at least one of a transition metal and post-transition metal. Moreover, metal oxides of the electrode can comprise at least one of a transition metal oxide and post-transition metal oxide. The electrode, for example, can have any composition and/or properties described herein. In some embodiments, the electrode is a mixture of metal oxides, such as chromium oxide and gallium oxide. The electrocatalytic site for reduction of CO_2 to CO may be anionic or exhibit anionic character, in some embodiments. Additionally, the electrocatalytic site may be selective to the reduction of CO_2 to CO in that the site does not participate in other redox chemistries. The electrode comprising an alloy and/or mixture of metal oxides may contain one or more additional electrocatalytic sites for producing other products. In some embodiments, for example, the electrode comprises a non-ionic site for the production of formate in addition to the electrocatalytic site for CO_2 reduction to CO.

[0021] These embodiments are further illustrated in the following non-limiting examples.

EXAMPLE 1 - *Ni_3Al Electrocatalytic Reduction of CO_2 to Oxygenated Organics*

[0022] Here it is shown that a Ni_3Al thin film electrocatalyst supported on glassy carbon can generate reduced C_1, C_2, and C_3 products from CO_2 with good performance, stability, and reproducibility at modest overpotential. Competing copper-based electrocatalysts were first reported to carry out the reduction of CO_2 to C_2 and C_3 products in 1988. For the first time it is demonstrated that metal alloys can generate C_3 products, electrocatalytic activity that, until now, has been uniquely associated with copper-based electrode systems. Further, the data presented here suggest that the Ni_3Al system is more stable than copper-based systems.

[0023] Ni_3Al thin film alloys were synthesized on glassy carbon substrates by adapting a drop-casting and furnace reduction procedure employed by Torelli et al., ACS Catal. 2016, 6, 2100-2104. As shown in FIG. 1, powder X-ray diffraction of the alloys confirmed the successful generation of the cubic Ni_3Al composition as indicated by the (111) and (211) planes; energy-dispersive X-ray spectroscopy supported the compositional analysis. X-ray photoelectron spectra (XPS) of a virgin (i.e. not utilized) electrode showed the presence of three Ni species: $Ni(OH)_2$, NiO, and Ni metal, with the Ni^{2+} components making up a majority of the composition, while all surface Al adopted the oxidized Al_2O_3 form. Thin films exhibited macroscopic surface areas of approximately 0.75 cm^2, while imaging by scanning electron microscopy, shown in FIG. 1, indicated that the films were comprised of micro-scale platelets uniformly distributed across the glassy carbon surface. In preliminary electrochemical experiments, cyclic voltammetry scans performed in aqueous electrolyte under CO_2 versus Ar saturation resulted in relatively featureless traces, although current enhancement was observed at more negative potentials leading into a proton reduction wave (FIG. 2A).

[0024] Bulk electrolysis experiments using the Ni_3Al thin film on glassy carbon as the working electrode and a Pt mesh counter electrode were performed at an applied potential of -1.38 V vs. Ag/AgCl in a sealed two-compartment cell containing 0.1 M K_2SO_4 electrolyte solution saturated with CO_2 (pH 4.5). Total current densities of -2.1 $\pm$ 0.4 mA/cm^2 were recorded and could be maintained for a period of several hours. ^{1}H-NMR spectra obtained as a function of electrolysis time (see FIG. 2B) indicated the growth of largely isolated peaks characteristic of 1-propanol (triplet; 0.73 ppm), acetone (singlet; 2.07 ppm), ethanol (triplet; 1.03 ppm), methanol (singlet; 3.20 ppm), and formate (singlet; 8.29 ppm) over time.

[0025] Several analytical methods were employed to confirm the identities of these C_1-C_3 products and to support the assertion that they were, in fact, derived from the CO_2 starting material. Electrolysis experiments performed using $^{13}CO_2$

yielded ^{1}H-NMR traces for 1-propanol, ethanol, methanol, and formate exhibiting the peak splitting expected for ^{13}C-coupling. However, a large doublet signal of 2-propanol (believed to be generated from acetone reduction) obscured the ethanol triplet, and acetone splitting was inconclusive using simple ^{1}H-NMR. To resolve these ambiguities ^{13}C-NMR spectra were obtained, resulting in the observation of a clear set of ethanol peaks (FIG. 2C). In addition, a ^{1}H-^{13}C heteronuclear single quantum correlation (HSQC) NMR experiment was performed to confirm the presence of ^{13}C-labelled acetone (FIG. 2D). Moreover, peak splitting within the ^{13}C-NMR spectrum, particularly in the C_2 and C_3 products, implied that all product carbon atoms were derived from the original $^{13}CO_2$ material. Mass spectrometry further supported the NMR results.

[0026] Faradaic efficiencies of 1.9 ± 0.3% for 1-propanol, 1.0 ± 0.2% for methanol, and 0.75 ± 0.03% for formate were observed, with lesser contributions from ethanol and trace amounts of acetone. As shown in FIG. 3A, the potential dependence of CO_2 electroreduction to these liquid products confirms -1.38 V vs. Ag/AgCl as the optimal potential at which to operate the electrochemical cell. The electrolyte pH was also found to strongly impact the overall CO_2 conversion efficiency and the distribution of products as summarized in FIG. 3B. Highest product yields were observed at pH~4.5. It is worth noting that the solution pH changes at most a few tenths of a unit from the beginning to the end of an electrolysis experiment. Given that all electrolysis experiments utilized efficient and continuous stirring of the electrolyte, the constant bulk value of the electrolyte pH suggests that any pH variation at the electrode surface was slight and, according to FIG. 3B, did not drastically alter the product distribution.

[0027] An understanding of the mechanism facilitated by the Ni_3Al film would allow for future work in optimizing the generation of select C_1, C_2, or C_3 products. As such, the headspace of the electrochemical cell following electrolysis was examined, and it was discovered that CO was the only gaseous CO_2 reduction product generated. Like the liquid products, CO production was maximized at -1.38 V vs. Ag/AgCl, at which point Faradaic efficiencies of 33 ± 3% were attained. As reported in FIG. 3B, the remainder of the gas generated was H_2. The fact that maximum liquid product and CO yields are achieved at the same applied potential suggests that CO might be an intermediate in CO_2 electroreduction to major products such as 1-propanol and methanol. To test this hypothesis, CO_2 was replaced with CO as the feedstock in electrolysis and examined the resulting reduction products by ^{1}H- NMR. Ni_3Al thin films on glassy carbon reduced CO to methanol as well as the C_2 and C_3 liquid products achieved using a CO_2 feedstock and in the same relative quantities. Electrolysis experiments utilizing a mixed $^{13}CO_2/^{12}CO$ feedstock indicated that 1-propanol, methanol, ethanol, and acetone were preferentially generated from CO, with only small contributions from $^{13}CO_2$. In these experiments, trace or no formate was produced.

[0028] Furthermore, plotting 1-propanol and methanol quantities obtained during CO-feedstock trials against the amount of charge passed during an experiment, as shown in FIGS. 4A and 4B, illuminated differences in rate of product generation. Specifically, when the electrochemical cell was saturated with CO_2, both 1-propanol and methanol increased linearly with charge passed. However, when the feedstock was switched to CO, though 1-propanol retained its linearity (but had a slope that was greater by two orders of magnitude than that of the CO_2-derived analog), methanol formation adopted an exponential growth curve.

[0029] Accordingly, it appears that CO is, in fact, an intermediate leading to Ni_3Al's generation of methanol, C_2, and C_3 products from CO_2. It is suggested that the reduction of CO_2 to CO is the limiting process in this electroreduction, leading to preferential use of CO as the reactant when both CO and CO_2 are present, as well as linear product generation curves when CO_2 is the available species being reduced. Only one CO_2 molecule, and therefore one CO molecule, must be present to produce methanol, so when the system is supplied with CO as the feedstock it generates methanol relatively easily, leading to an exponential production curve. The generation of 1-propanol necessitates the presence of three carbon atoms, so even if the limiting step is removed by providing CO as the reactant, accumulation of three CO molecules near one another on the thin film surface is still required. Thus, the linear trend for 1-propanol remains, though its slope increases because the CO_2 to CO conversion step has been eliminated. This sort of mechanistic analysis, though preliminary, will help to improve the design and optimization of future alloy catalysts.

[0030] The fact that Ni_3Al generates quantifiable amounts of C_3 products, alongside useful C_1 and C_2 products, is interesting because of the thin film's stability, reproducibility, and modest overpotential. It is worth noting that, upon cursory examination of the related intermetallic NiAl, significantly diminished Faradaic efficiencies were achieved for the products described herein. The previously reported Ni-Ga thin film system plated on a highly oriented pyrolytic graphite substrate achieved maximum Faradaic efficiencies for C2 products of approximately 1.7% and 0.4% for ethane and ethylene, respectively, with no indication of C3 product formation. Methane was also observed. Faradaic efficiency of 1.9 ± 0.3% for the C_3 product 1-propanol indicates a heterogeneous synthetic route to higher order organic compounds that has not previously been reported at alloy electrode interfaces.

[0031] The inventors have recently suggested a catalytic efficiency parameter that serves to summarize both the overpotential and turnover frequency (catalytic current) of an electrocatalytic reaction independent of mechanistic details. This single parameter allows one to compare a variety of catalysts that transform a given substrate to the same product. Ni_3Al catalytic efficiency parameter for 1-propanol generation is calculated to be 0.5 ± 0.1%. This is comparable to the catalytic efficiency parameter for Torelli *et al.*'s Ni-Ga thin film in the generation of ethane (0.44%; based on maximum

Faradaic efficiency), their major C2 product.

[0032] Furthermore, it is well established that copper electrodes suffer from instability in solution and excessive overpotential requirements for the formation of higher order organic products, making their usage to-date impractical. Ni_3Al, on the other hand, is stable in aqueous solution over the time scale explored here. This work shows that Ni_3Al generates electroreduced products from CO_2 continuously over a period of four to five days. Scanning electron microscopy confirms that the thin film is robust and, as demonstrated by the small amount of material loss observed, withstands exposure to electrochemical conditions while maintaining initial efficiencies for CO_2 reduction. This finding is supported by post-electrolysis XPS analysis demonstrating that the electrode surface composition remains unchanged during electrochemical CO_2 reduction.

[0033] The Ni_3Al thin film on glassy carbon reported here is the first copper-free, heterogeneous electrocatalyst capable of generating C_3 products, including 1-propanol and acetone, from CO_2 starting material, and its Faradaic efficiencies for 1-propanol generation are competitive with those achieved on most copper electrodes. Ultimately, these significant factors suggest that heterogeneous catalysts comprised of metals other than copper may generate highly reduced products from CO_2 whose identities, Faradaic efficiencies, selectivities, or overpotentials rival or exceed those achieved on copper catalysts.

Methods

[0034] Thin film Ni_3Al alloys were synthesized as previously described.[19] Briefly, aqueous solutions of 0.052 M nickel(II) nitrate hexahydrate and 0.036 M aluminum(III) nitrate nonahydrate were combined in appropriate ratios to achieve the Ni_3Al stoichiometry. In 0.1-mL increments, 0.5-mL portions of the nickel-aluminum nitrate solution were drop-casted onto glassy carbon pieces that had been set on a hot plate and heated to 150 °C. After drop-casting, the substrates remained on the hot plate for 15 min until the solution completely evaporated, revealing green surface films. The substrates were then placed in alumina boats and loaded into either a Lindberg/Blue M or Carbolite Quartz Tube Furnace under 95% Ar/5% H_2 gas flow. The furnace was ramped at a rate of 3 °C/min to 700 °C, where it rested for 5 h.

[0035] Electrodes were prepared by affixing a coiled copper wire to the glassy carbon substrate using conducting silver epoxy, extending the length of copper wire through a glass tube, and sealing both ends of the tube using insulating epoxy. It was critical that the insulating epoxy was also used to completely cover the silver epoxy and copper wire attached to the substrate. In some experiments, the top of a film-deposited substrate was wrapped in copper tape and held using an alligator clip attached to copper wire similarly threaded through a glass tube sealed with insulating epoxy. Comparable amounts of charge were passed in electrochemical experiments featuring the two types of electrode preparations.

[0036] Electrochemical experiments were performed using CH Instruments 760 and 1140 potentiostats. Cyclic voltammetry experiments were completed in a three-neck round-bottom flask using the Ni_3Al film on glassy carbon as the working electrode referenced to Ag/AgCl and a Pt mesh counter electrode in 0.1 M K_2SO_4 at pH 4.5. Bulk electrolysis experiments were undertaken in the same electrolyte solution (with the exception of pH dependence experiments, which utilized K_2SO_4 buffered with $KHCO_3/CO_2$) using custom electrolysis cells with gas-tight ports for the above electrodes. In these experiments, the Pt mesh counter electrode was situated in a fritted gas dispersion tube to separate the reduction reaction at the cathode from oxidation processes at the anode, and a stir bar was employed. The reaction solutions were purged with CO_2, CO, or Ar for 20 min prior to experimental or control trials; experiments using $^{13}CO_2$ were not completely purged with the starting material, resulting in a small amount of $^{12}CO_2$ contamination that could be quantified by ^{1}H-NMR. Bulk electrolysis experiments were performed over intervals of at least 4 h, during which time the headspace was sampled every 20 min and the electrochemical solution was sampled every 60 min. During and after bulk electrolysis experiments, both the solution and headspace were sampled for products using ^{1}H- or ^{13}C-NMR (referenced to 1,4-dioxane internal standard) and gas chromatography, respectively.

EXAMPLE 2 - *Cr_2O_3-Ga_2O_3 Electrocatalytic Reduction of CO_2 to Oxalate*

[0037] In this example, an electrode composed of a chromium oxide-gallium oxide thin film on glassy carbon is employed to transform CO_2 to oxalate in water. To our knowledge, this is the first heterogeneous electrocatalyst system capable of transforming CO_2 to oxalate in water, introducing new possibilities for catalyst discovery and tangible opportunities for the energy efficient conversion of CO_2 to a chemical feedstock containing more than one carbon.

[0038] Thin films of Cr-Ga (3:1 ratio) on glassy carbon solid supports were synthesized using a drop-casting and thermal reduction method adapted from Torelli et al, Nickel-gallium-catalyzed electrochemical reduction of CO2 to highly reduced products at low overpotentials. ACS Catal. 6, 2100-2104 (2016). Powder X-ray diffraction (XRD; FIG. 5A) coupled with energy-dispersive X-ray spectroscopy suggested that the bulk films were comprised of Cr_2O_3 and Ga_2O_3 in the desired 3:1 stoichiometry. Surface compositions were analyzed by X-ray photoelectron spectroscopy (FIG. 5B), which pointed to an oxidized surface comprised of mostly Cr(III), matching the bulk, and Ga oxides. Scanning electron

microscopy (FIG. 1A) indicated that Cr_2O_3-Ga_2O_3 films were comprised of discontinuous platelets scattered across the glassy carbon surface, not unlike alternative bimetallic systems similarly synthesized.

[0039] Initial bulk electrolysis experiments were conducted using a Pt mesh counter electrode and 0.1 M KCl electrolyte (pH 4.1 after CO_2 purging). Applying a potential of -1.38 V vs. Ag/AgCl to an electrochemical cell purged with $^{13}CO_2$ induced generation of CO and H_2, sampled by gas chromatography, as well as oxalate, formate and methanol, detected in the liquid phase by ^1H and ^{13}C-NMR. A high-intensity peak at 161 ppm overshadowed formate, methanol, and residual CO_2 signals and was assigned to oxalate. To confirm this product assignment, a sample of the electrolyzed solvent which had been treated with HCl to remove any carbonate present was mixed with calcium bromide, causing precipitation of a white solid which was isolated by vacuum filtration and examined by infrared (IR) spectroscopy (FIG. 6). Only IR transitions associated with calcium oxalate were observed.

[0040] In order to optimize the Cr_2O_3-Ga_2O_3 system for oxalate production, pH, electrolyte, potential dependence, and stoichiometric studies were undertaken. Gravimetric determination of oxalate is well established and was found to be quantitative in the present study when a 1 M calcium bromide solution was utilized on post electrolysis samples. Standard curves were employed for quantifying CO/H_2 and formate/methanol using gas chromatography and ^1H-NMR, respectively.

[0041] All pH-varying experiments were conducted at an applied potential of -1.38 V vs. Ag/AgCl and used CO_2-saturated KCl electrolyte (buffered with $KHCO_3$ for pH > 4; adjusted with HCl for pH < 4; 0.1 M concentration). As shown in FIG. 7, the Cr_2O_3-Ga_2O_3 system is only slightly sensitive to solution pH, since statistically equivalent oxalate Faradaic efficiencies were achieved at pH 4.1 and 5.1, while pH 6.1 yielded slightly inferior results. Markedly lower Faradaic efficiencies at pH 7.1 suggest that carbonate is not involved in oxalate production, as these experiments contained the highest original concentration of $KHCO_3$ buffer. Charge balance was achieved in all cases by H_2 generation.

[0042] In separate experiments, the electrolyte anion was varied (i.e., KCl, KBr, and KI were compared), since other researchers have reported that CO_2 reduction product selectivity can be highly electrolyte dependent. However, in the Cr_2O_3-Ga_2O_3 system, carbon-containing products did not exhibit this dependence. Subsequent experiments therefore utilized CO_2-saturated, pH 4.0 KCl, because this pH maximized total Faradaic efficiency for carbon-containing products compared to H_2. Furthermore, bulk solution pH consistently rose to 4.5-5.0 by the end of electrolysis (when initial pH = 4.1), and as shown in Fig. 7, maximum oxalate Faradaic efficiencies would still be achieved at these final pH conditions.

[0043] Subsequently, potential dependence experiments were conducted using the optimized electrolyte conditions. Notably, all potentials examined resulted in some oxalate generation, despite being significantly more positive than the thermodynamic potential required for one-electron reduction of CO_2 to $CO_2^{\cdot-}$, the intermediate that has historically been invoked for the conversion of CO_2 to oxalate. The resulting Faradaic efficiencies, displayed in Fig. 8, suggest that the Cr_2O_3-Ga_2O_3 system is more sensitive to applied potential than pH. Additionally, the two major carbon-containing products, oxalate and CO, reached maximum efficiencies at different potentials. An electrode potential of -1.48 V vs. Ag/AgCl (630 mV more positive than E° for reducing CO_2 to $CO_2^{\cdot-}$) was determined to be the optimal potential for oxalate production.

[0044] A cell employing 0.1 M KCl (pH 4.0) at a potential of -1.48 V vs. Ag/AgCl, generated Faradaic efficiencies for oxalate, CO, formate, and methanol of 59 $\pm$ 3%, 8.1 $\pm$ 0.7%, 0.16 $\pm$ 0.02%, and 0.15 $\pm$ 0.02%, respectively. Materials characterization post-electrolysis suggested that Cr_2O_3-Ga_2O_3 system continued to be chemically and physically stable. XPS analysis revealed only subtle changes in surface composition. Surface Cr remained more than 99% Cr(III), in agreement with the Cr Pourbaix diagram. Still, Ga metal did not make up the majority of the sample, but its XPS spectrum largely resembled its pre-electrolysis analog, confirming a stable surface. SEM imaging indicated that the thin film incurred only slight erosion at platelets' edges during electrolysis, while EDX showed that the 3:1 Cr:Ga stoichiometry was maintained. A single Cr_2O_3-Ga_2O_3/glassy carbon electrode could transform CO_2 continuously for more than 10 days (the longest time period studied), suggesting an attractive catalytic lifetime.

Determination of reaction intermediates en route to oxalate

[0045] The Cr_2O_3-Ga_2O_3 film on glassy carbon is a promising catalyst due to its high oxalate Faradaic efficiency, good stability, and, perhaps most interestingly, its ability to perform the electrochemical transformation in water. At the applied potentials studied here, ranging from 530 to 930 mV more positive than the E° required for $CO_2^{\cdot-}$ generation, CO_2 reduction to oxalate cannot occur through a $CO_2^{\cdot-}$ intermediate, which means a pathway as-yet unreported for the electrochemical CO_2-to-oxalate transformation must be at play. While prior studies often rely on the supposition of a $CO_2^{\cdot-}$ intermediate, calculations have been performed evaluating a homogeneous catalytic system, consisting of a dinuclear Cu complex in acetonitrile solvent, that explicitly refute a $CO_2^{\cdot-}$-dependent pathway in that case. To determine whether any of the alternative CO_2 reduction products serve as intermediates en route to oxalate, a series of electrolysis experiments were performed, which replaced the CO_2 feedstock with CO, formate, methanol, or combinations of these carbon-containing compounds.

[0046] Ultimately, during electrolysis experiments conducted using the optimized pH, electrolyte, and potential plus ^{13}CO and methanol (rather than CO_2), oxalate was produced, as confirmed by precipitation with calcium bromide as

well as ^{13}C-NMR. This ^{13}CO experiment, which used ^{12}C-methanol, also verified that CO was incorporated into the oxalate product. The opposite labeling experiment, using ^{12}CO and ^{13}C-methanol, was also undertaken, resulting in no ^{13}C-NMR signal even though calcium oxalate was precipitated out of solution. Therefore, methanol is not incorporated into the product. Significantly, supplying Cr_2O_3-Ga_2O_3 with either CO or methanol, rather than both, does not result in an oxalate end product; both species are required even though only the CO ends up in the reaction product. Rather than a $CO_2^{\cdot-}$-dependent pathway, Cr_2O_3-Ga_2O_3 production of oxalate therefore appears to rely on CO and methanol, which it can first generate from CO_2.

[0047] The incorporation of CO and use of short-chain alcohols in oxalate generation is not unprecedented, although it has not previously been accomplished using a CO_2 starting material. Large-scale manufacture of oxalate is frequently accomplished by oxidative carbonylation of small alcohols to achieve diesters of oxalic acid, followed by hydrolysis to attain the oxalate product. This reaction consumes O_2 to re-oxidize the catalyst, which can be a two-component metal system, such as Pd plus $FeCl_2$ or $CuCl_2$.

[0048] FIG 9 illustrates Faradaic efficiencies of carbon-containing products. While oxalate generation is generally suppressed at high KCl concentrations, low CO and high formate Faradaic efficiencies contribute to decreased oxalate production at low KCl concentrations. Electrolyses were performed at -1.48 V vs. Ag/AgCl. In feedstock experiments, formate was shown to be a competitor of, rather than intermediate contributing to, oxalate production.

[0049] Cr_2O_3-Ga_2O_3 methods of generating oxalate exhibit critical mechanistic differences with oxidative carbonylation processes, which could make Cr_2O_3-Ga_2O_3 a more attractive option for oxalate synthesis. Ultimately, the Cr_3Ga catalyst introduces a new and practical means of generating oxalate from CO_2, but it also demonstrates that electrochemical routes excluding a $CO_2^{\cdot-}$ intermediate are not only possible but can operate both in aqueous environments and at much lower applied potentials than previously thought.

[0050] Such a departure from the previously accepted mode of CO_2 reduction to oxalate invites a question about the roles of the metals within the Cr_2O_3-Ga_2O_3 catalyst. To answer that question, the pure metal films as electrocatalysts were first examined. At -1.48 V vs. Ag/AgCl (pH 4.0 KCl), films of Cr on glassy carbon generated modest amounts of CO, formate, and methanol from CO_2, while the activity of Ga films was dominated by CO production at around 40% Faradaic efficiency. Regardless, plain Ga thin films converted about 20% of the CO_2 in the system to carbonate, observable on the surface post-electrolysis by XPS, while Cr's carbonate production was more limited. As thin films, neither metal alone could produce oxalate from CO_2, confirming the importance of having both metals present.

[0051] A clear need for both Cr and Ga implies that an optimal Cr:Ga stoichiometry exists for maximizing oxalate production. To determine this stoichiometry and gain additional insight into the role of each metal, a range of stoichiometries spanning from 100% Cr to 100% Ga were synthesized as thin films on glassy carbon and analyzed for their performance as CO_2 reduction electrocatalysts. All experiments were conducted at -1.48 V vs. Ag/AgCl in 0.1 M KCl (pH 4.05) for comparison to the optimized oxalate outcome for Cr_2O_3-Ga_2O_3.

[0052] The trends in carbon-containing product generation based on Cr:Ga stoichiometry are displayed in Fig. 10. Cr_2O_3-rich stoichiometries corresponded to lower overall quantities of non-oxalate products compared to Ga-rich variants, but, most notably, Faradaic efficiencies for CO (essential for oxalate generation) reached their lowest values at the highest percentages of Cr. The highest Faradaic efficiency for oxalate was obtained at the original 3Cr:IGa stoichiometry. When considering the product trends in FIG. 10, it seems that optimal oxalate generation requires ideal combinations of CO/methanol production and formate suppression. Some critical quantity of Cr is needed to ensure that oxalate is produced efficiently, but excess Cr prevents adequate generation of CO, which decreases oxalate Faradaic efficiencies. Complementarily, Ga seems to be the major CO-generating component of the system. In combination, these factors make Cr_2O_3-Ga_2O_3 one preferred embodiment for oxalate production, with the recognition that oxalate production can be achieved with other electrode compositions, systems and methods described herein. Other alloys and/or oxides thereof exhibiting the mechanistic requirements described herein may be employed for oxalate production.

[0053] The ability of the Cr_2O_3-Ga_2O_3 thin film on glassy carbon to generate oxalate from CO_2 in water makes it a landmark example of heterogeneous CO_2 electroreduction, as previous studies of this conversion were confined to use of nonaqueous electrolytes and applied potentials reflective of a $CO_2^{\cdot-}$ intermediate. With optimal electrolysis conditions of pH 4.0 aqueous KCl and -1.48 V vs. Ag/AgCl, the pathway used to generate oxalate by this system must not include $CO_2^{\cdot-}$ coupling. Instead, CO_2 is reduced to CO and methanol, which are then used to produce oxalate.

[0054] Oxalate Faradaic efficiencies of 59 $\pm$ 3% and initial lifetime studies exceeding 10 days of continuous use show the potential for Cr_2O_3-Ga_2O_3 as a candidate catalyst for a new industrial oxalate process, especially because it achieves the desired end product using aqueous solution, atmospheric pressure, and CO_2 starting material.

Nature of Cr-Ga Surface Sites Active in CO_2 Reduction

[0055] Notably, the reactant experiments that initially pointed to oxalate-generating roles for CO and methanol did not implicate an important role for formate, which has been indicated as a competitor of oxalate production in the literature. With a Cr-Ga electrode, use of a formate feedstock resulted in only trace amounts of methanol and failed to generate

oxalate. This result suggested that distinct active sites may exist for generation of formate and CO-derived products, including oxalate. Further support for this prediction was provided by electrolyte dependence studies. While experiments varying the electrolyte anion (i.e., KCl, KBr, KI, K_2SO_4, and KH_2PO_4) failed to exhibit significant differences in the distribution of products, a stark dependence was noted when varying the electrolyte cation.

[0056] Use of LiCl or NH_4Cl electrolytes (0.1 M) and -1.48 V vs. Ag/AgCl applied potential resulted in similar product distributions and efficiencies as those recorded for KCl. However, analogous experiments using CsCl, $(CH_3)_4NCl$ ((TMA)Cl), and $CaCl_2$ electrolytes failed to generate any detectable quantities of oxalate, and CO Faradaic efficiencies were also reduced. (TMA)Cl supporting electrolyte increased the Faradaic efficiency of formate to 7.7 ± 0.4%, compared to the 0.16 ± 0.02% value achieved using optimal oxalate-generating conditions (0.1 M KCl). These cation-dependence results are summarized in Table 2.

Table 2 – Products generated according to electrolyte cation identity

Electrolyte cation	Faradaic efficiency (%)†			
	Oxalate	*CO*	*Formate*	*Methanol*
Li^+	47 ± 4	13.6 ± 0.8	0.13 ± 0.04	0.08 ± 0.02
K^+	59 ± 3	8.1 ± 0.7	0.16 ± 0.02	0.15 ± 0.02
NH_4^+	43 ± 5	6.6 ± 0.4	0.20 ± 0.05	0.17 ± 0.03
Cs^+	0	3.6 ± 0.5	4.2 ± 0.3	0.21 ± 0.03
TMA^+	0	1.8 ± 0.5	7.7 ± 0.4	0.95 ± 0.07
Ca^{2+}	0	3.7 ± 0.6	5.1 ± 0.4	0.52 ± 0.03

†Standard deviation based on the average of two trials.

Furthermore, Cr-Ga electrodes previously used in (TMA)Cl experiments did not regain their oxalate-generating ability when re-introduced into a KCl-containing electrolyte. This KCl electrolyte was subjected to ^{1}H-NMR after electrolysis, and the resultant spectrum exhibited an overwhelming signal from TMA^+, which must have come from the Cr-Ga surface. TMA^+ had therefore chemisorbed to the catalyst during prior electrolyses, likely contributing to inhibition of oxalate generation in those and subsequent experiments. Formate generation remained higher than usual in these trials.

[0057] Exacerbation of formate production when oxalate generation is suppressed further supports the proposal that at least two surface active sites are present in the Cr-Ga catalyst: one for CO and CO-derived productions and a second for formate. Moreover, chemisorption of TMA^+ onto the Cr-Ga surface suggests that a surface anion is present, while lack of oxalate production in the presence of cations having few waters of hydration (TMA^+ and Cs^+) or strong anion-binding capacity (Ca^{2+}) hints that this surface anion is critical to CO/oxalate generation. To probe this theory, the Cr-Ga system (0.1 M KCl, -1.48 V vs. Ag/AgCl) was treated with 15 mM NaCN prior to electrolysis, anticipating that the Lewis-basic, anionic CN^- ligand would bind specifically to a Lewis-acidic, non-anionic surface site. Indeed, after performing electrolysis with this modified system, CO, oxalate, and methanol were detected in typical yields, while no formate was produced. Thus, it appears that the CN^- ligates the formate-generating active site, simultaneously demonstrating that this site is (A) chemically distinct from the CO-generating site and (B) not anionic in character. This experiment, combined with the cation-dependence data, strongly suggests that Cr-Ga contains two types of electrocatalytic surface sites for CO_2 reduction: an anionic site leading to CO-derived products and a non-anionic site that produces formate.

Materials and Methods

Materials

[0058] Chromium(III) nitrate nonahydrate (>_ 99.99%), gallium(III) nitrate hydrate (99.9%), $KHCO_3$ (99.7%), oxalic acid (>_ 99%), NH_4Cl (99.998%), $(CH_3)_4NCl$ ((TMA)Cl; ≥ 98%), NaCN (97%), methanol (≥ 99.9%), ^{13}C-methanol (99 at% ^{13}C), formic acid (>_ 98%), 1,4-dioxane (99.8%), acetonitrile (99.8%), ethanol (≥ 99.8%), isopropanol (≥ 99.7%), $^{13}CO_2$ (99 at% ^{13}C), ^{12}CO (^{13}C-depleted), and ^{13}CO (99 at% ^{13}C) were obtained from Sigma-Aldrich. KCl, KBr, KI, K_2CO_3, K_2SO_4, KH_2PO_4, LiCl, CsCl, $CaCl_2$, and HCl, all ACS grade, were purchased from EMD Chemicals, and calcium bromide (99.5%) was obtained from Alfa Aesar. Ar, CO_2, CO, 95% Ar/5% H_2, and 50% CO/50% H_2 gases and mixtures were ordered from AirGas. Glassy carbon plates (GLAS11; 25 x 25 x 3 mm; Structure Probe Inc.) were cut in half lengthwise prior to use. Conducting silver and Loctite Hysol insulating epoxies were purchased from Epo-Tek and

Grainger, respectively. All chemicals were used as received except for methanol and formic acid for standard curves, 1,4-dioxane for NMR internal standards, and HCl, all of which were diluted prior to use.

Methods

[0059] Synthetic procedures to create Cr-Ga thin films of various stoichiometries are described. Aqueous solutions of 0.052 M chromium(III) nitrate nonahydrate and 0.036 M gallium(III) nitrate hydrate were mixed to achieve the desired Cr:Ga ratio. Glassy carbon pieces were heated to ~120 °C on a hotplate, and 0.1-mL samples of the Cr-Ga nitrate solution were drop-casted onto them. After the solution evaporated completely, the glassy carbon pieces were placed in an alumina boat and loaded into either a Lindberg/Blue M or Carbolite Quartz Tube Furnace. The furnace was ramped at a rate of 3 °C/min to 700 °C under 95% Ar/5% H_2 gas flow; it rested at this state for 5 h prior to cooling to room temperature at a rate of -3 °C/min. Resulting Cr-Ga films were olive green in color, with Cr-rich stoichiometries tending toward kelly green and Ga-rich stoichiometries tending toward gray.

[0060] Electrodes were prepared in one of two fashions. One electrode configuration involved connecting copper wire to the glassy carbon support using conducting silver epoxy, feeding the wire through a glass tube, and covering both ends of the tube (including any exposed copper or silver) with insulating epoxy. The second configuration featured the same general setup, but the copper wire was attached to an alligator clip, which could then be used to reversibly hold glassy carbon pieces whose tops had been wrapped in copper tape. Experiments using both electrode configurations yielded identical results, both in terms of charge passage and product distribution.

[0061] Electrochemical experiments were conducted using CH Instruments 760 and 1140 potentiostats. Bulk electrolysis experiments utilized custom electrochemical cells with gas-tight ports for the working, Pt mesh counter (situated in a gas dispersion tube), and Ag/AgCl reference electrodes. The electrolyte was continuously stirred. Unless otherwise noted, 0.1 M KCl was used as the electrolyte, and it was buffered with $KHCO_3$ to achieve CO_2-saturated pH values > 4 or adjusted with 0.01 M HCl for values < 4. Electrolyte solutions were purged with CO_2 for 30 min prior to experimentation. In experiments without CO_2 (i.e., CO, formic acid, methanol, or combinatorial feedstocks), the pH was adjusted to the appropriate, CO_2-analogous value. The majority of electrolyses were conducted at pH 4.1, and post-electrolysis measurements indicated that the final solution pH was consistently between 4.5 and 5.0. Experiments using $^{13}CO_2$, ^{13}CO, and ^{12}CO (^{13}C-depleted) were not completely purged with the respective gas.

[0062] Electrolysis experiments were performed until 30-40°C charge had passed, unless the experiment was meant to determine catalyst lifetime. The solution and headspace of electrochemical cells were sampled for liquid and gaseous products by ^1H-NMR (referenced to 1,4-dioxane internal standard) and gas chromatography, respectively, both during and after bulk electrolysis. Oxalate was detected by ^{13}C-NMR and quantified by precipitation of the calcium salt.

Cr-Ga Thin Film Characterization

[0063] The compositions and morphologies of Cr-Ga films were analyzed by a variety of materials characterization techniques. Powder X-ray diffraction was performed using a Bruker D8 Advance diffractometer with 0.083° step size and CuKα radiation. XRD samples either remained on the glassy carbon support or were scraped from the surface; resulting patterns were identical, except that scraped samples exhibited significantly less carbon intrusion and were therefore selected for presentation herein. Thin film morphology and additional bulk composition data were obtained using a FEI XL30 FEG-SEM equipped with EVEX EDS detector. SEM images and EDX spectra were obtained using a 5 or 10 keV electron beam with a 10-15 mm working distance. XPS spectra were collected using a ThermoFisher K-Alpha X-Ray Photoelectron Spectrometer set to 20 eV pass energy and 50 ms dwell time. Resulting data were analyzed using the Thermo Scientific Avantage Data System and CasaXPS software. Materials characterization was conducted before and after electrochemistry in designated experiments.

Product Analysis

[0064] Formate and methanol were detected by ^1H-NMR after combining 530 μL electrolyte with 60 μl D_2O and 10 μL 1,4-dioxane (10 mM); the latter served as an internal standard. In ^{13}C-NMR experiments (used primarily to detect oxalate), only 1 μL 1,4-dioxane (10 mM) was added. A Bruker Avance III 500 MHz NMR Spectrometer with cryoprobe detector was used for all NMR experiments, and the experiments incorporated a custom water suppression method to permit sampling of aqueous electrolyte solutions. Formate and methanol were quantified using 5-point calibration curves for ^1H-NMR, while oxalate was visualized qualitatively by a large ^{13}C-NMR signal (in experiments utilizing ^{13}C-labeling) in the 160-170 ppm range.

[0065] Oxalate was quantified by first treating a sample of the electrolysis solution with 1 M HCl (to remove any carbonate byproduct) and then adding 1 M calcium bromide solution, which resulted in the precipitation of calcium oxalate. The calcium oxalate sample was dried in an oven at 105 °C overnight and then massed; this mass was used

to calculate the total quantity of oxalate. IR spectra of calcium oxalate samples were obtained using a Thermo Diamond Smart Orbit IR Spectrometer set at 1 cm^{-1} resolution. The carbonate byproduct could be quantified by finding the difference in mass between two electrolysis samples, one treated with HCl and the other untreated prior to calcium bromide addition; the difference in mass was attributed to calcium carbonate, which was then calculated as a percentage of the total CO_2 in solution (based on the electrolyte volume unique to each experiment). Calcium carbonate was also examined by IR spectroscopy. Experimental calcium oxalate and calcium carbonate samples were compared to control compounds made by combining calcium bromide and either oxalic acid or K_2CO_3 in aqueous solution.

[0066] Headspace samples were analyzed by gas chromatography for gaseous products. CO was measured using a HP6890 Gas Chromatograph fitted with a Molsieve 5A PLOT capillary column (Agilent) and TCD. The sampling method was a 5-min, 60 °C isotherm with He flow gas. An SRI 8610C Gas Chromatograph with Ar flow, which also used a Molsieve column and TCD, was run for a 7-min isotherm at 80 °C to detect H_2. CO and H_2 were quantified using 30-point calibration curves having R^2 values ≥ 0.99. The headspace was also sampled following $^{13}CO_2$ electrolyses using a KBr-terminated gas cell and Nicolet iS50 FT-IR Spectrometer with 1 cm^{-1} resolution; this confirmed that the CO product was derived from CO_2. Faradaic efficiencies for all products, gaseous and liquid, were calculated based on the charge passed during each experiment as well as the product quantities determined by gas chromatography, ^{1}H-NMR, or calcium bromide precipitation. Catalytic efficiencies were calculated based on the following equation:

$$\text{Catalytic efficiency} = \frac{\text{Faradaic efficiency}}{\left(1+\frac{\text{overpotential}}{E^{\circ\prime}_{\text{product}}}\right)} \times 100\% \qquad \textit{Eqn. 1}$$

[0067] Various embodiments of the invention have been described in fulfillment of the various objects of the invention. It should be recognized that these embodiments are merely illustrative of the principles of the present invention. Numerous modifications and adaptations thereof will be readily apparent to those skilled in the art without departing from the scope of the invention.

[0068] The following features of the invention were claimed in the parent application and are presented here for basis of the current claims and for possible future amendments or divisional applications.

Feature 1. A system for providing oxygenated organic products comprising:
an electrochemical cell including an electrolyte solution comprising CO_2, and a working electrode comprising a transition metal/post transition metal (TM/PTM) binary alloy and/or oxide(s) thereof for electrocatalytic reduction of the CO_2 to the oxygenated organic products, wherein the oxygenated organic products comprise two or more carbon atoms and/or two or more oxygen atoms.

Feature 2. The system of Feature 1, wherein the TM/PTM binary alloy is of the formula TM_xPTM_y, and x and y are integers independently selected from 1 to 10.

Feature 3. The system of Feature 1, wherein the TM is a first row transition metal.

Feature 4. The system of Feature 1, wherein the PTM is selected from Group IIB or IIIA of the Periodic Table.

Feature 5. The system of Feature 1, wherein the electrolyte solution further comprises CO.

Feature 6. The system of Feature 1, wherein the oxygenated organic products comprise oxalate.

Feature 7. The system of Feature 1, wherein the TM is selected from Group VIIIB and the PTM is selected from group IIIA of the Periodic Table.

Feature 8. The system of Feature 7, wherein the TM is nickel and the PTM is aluminum.

Feature 9. The system of Feature 1, wherein the TM is chromium and the PTM is selected from Group IIIA of the Periodic Table.

Feature 10. The system of Feature 1, wherein transition metal oxide/post transition metal oxide comprises Cr_2O_3-Ga_2O_3.

Feature 11. The system of Feature 1, wherein the electrolyte solution has an acidic pH.

Feature 12. A system for providing oxygenated organic products comprising:
an electrochemical cell including an electrolyte solution comprising CO_2, and an electrode comprising an alloy and/or mixture of metal oxides, the electrode having an electrocatalytic site for reduction of CO_2 to a CO, wherein the CO is incorporated into the oxygenated organic products.

Feature 13. The system of Feature 12, wherein the alloy comprises at least one of a transition metal and post-transition metal.

Feature 14. The system of Feature 12, wherein the metal oxides comprise at least one of a transition metal oxide and post-transition metal oxide.

Feature 15. The system of Feature 14, wherein the transition metal oxide comprises a first row transition metal.

Feature 16. The system of Feature 14, wherein the post-transition metal oxide comprises a metal selected from group IIB or IIIA of the Periodic Table.

Feature 17. The system of Feature 12, wherein the mixture of metal oxides comprise chromium oxide and gallium oxide.

Feature 18. The system of Feature 12, wherein the oxygenated organic products comprise oxalate.

Feature 19. The system of Feature 12, wherein the electrolyte solution has an acidic pH.

Feature 20. The system of Feature 12, wherein the electrocatalytic site is anionic.

Feature 21. A system for providing organic products comprising:
an electrochemical cell including an electrolyte solution comprising CO_2, and a working electrode comprising a transition metal/post-transition metal (TM/PTM) binary alloy and/or oxide(s) thereof for electrocatalytic reduction of the CO_2 to the organic products.

Feature 22. The system of Feature 21, wherein the organic products comprise one carbon atom, two carbon atoms, three carbon atoms or mixtures thereof.

Feature 23. The system of Feature 21, wherein the organic products are oxygenated.

Feature 24. The system of Feature 21, wherein the organic products are aliphatic.

Feature 25. The system of Feature 21, wherein the TM/PTM binary alloy is of the formula TM_xPTM_y, and x and y are integers independently selected from 1 to 10.

Feature 26. The system of Feature 21, wherein the TM is a first row transition metal.

Feature 27. The system of Feature 26, wherein the PTM is selected from Group IIB or IIIA of the Periodic Table.

Feature 28. The system of Feature 21, wherein transition metal oxide/post transition metal oxide comprises Cr_2O_3-Ga_2O_3.

Feature 29. A method of forming oxygenated organic products comprising:

providing an electrochemical cell including an electrolyte solution comprising CO_2, and a working electrode comprising a transition metal/post transition metal (TM/PTM) binary alloy and/or oxide(s) thereof; and
electrocatalytically reducing the CO_2 to the oxygenated organic products, wherein the oxygenated products comprise two or more carbon atoms and/or two or more oxygen atoms.

Feature 30. The method of Feature 29, wherein the TM/PTM binary alloy is of the formula TM_xPTM_y, and x and y are integers independently selected from 1 to 10.

Feature 31. The method of Feature 29, wherein the TM is a first row transition metal.

Feature 32. The method of Feature 29, wherein the PTM is selected from Group IIB or IIIA of the Periodic Table.

Feature 33. The method of Feature 29, wherein the oxygenated organic products comprise oxalate.

Feature 34. The method of Feature 29, wherein transition metal oxide/post transition metal oxide comprises Cr_2O_3-Ga_2O_3.

Feature 35. A method of forming oxygenated organic products comprising:

providing an electrochemical cell including an electrolyte solution comprising CO_2, and an electrode comprising an alloy and/or mixture of metal oxides; and
reducing CO_2 to CO at an electrocatalytic site on the electrode; and
deriving the oxygenated organic products from the CO.

Feature 36. The method of Feature 35, wherein the oxygenated products comprise oxalate.

Feature 37. The method of Feature 35, wherein the metal oxides comprise at least one of a transition metal oxide and post-transition metal oxide.

Feature 38. The method of Feature 37, wherein the transition metal oxide comprises a first row transition metal.

Feature 39. The method of Feature 37, wherein the post-transition metal oxide comprises a metal selected from group IIB or IIIA of the Periodic Table.

Feature 40. The method of Feature 35, wherein the mixture of metal oxides comprise chromium oxide and gallium oxide.

Feature 41. The method of Feature 35, wherein the electrocatalytic site is anionic.

Feature 42. The method of Feature 35, wherein the electrolyte solution has acidic pH.

Claims

1. A system for providing oxygenated organic products comprising:
an electrochemical cell including an electrolyte solution comprising CO_2, and a working electrode comprising a transition metal/post transition metal binary alloy for electrocatalytic reduction of the CO_2 to the oxygenated organic products, wherein the oxygenated organic products comprise two or more carbon atoms and/or two or more oxygen atoms.

2. The system of claim 1, wherein the transition metal/post transition metal binary alloy is of the formula TM_xPTM_y, and x and y are integers independently selected from 1 to 10.

3. The system of claim 1, wherein the transition metal is a first row transition metal.

4. The system of claim 1, wherein the post transition metal is selected from Group 12 or 13 of the Periodic Table.

5. The system of claim 1, wherein the electrolyte solution further comprises CO.

6. The system of claim 1, wherein the oxygenated organic products comprise oxalate.

7. The system of claim 1, wherein the transition metal is selected from Groups 8-10 and the post transition metal is selected from group 13 of the Periodic Table.

8. The system of claim 7, wherein the transition metal is nickel and the post transition metal is aluminum.

9. The system of claim 1, wherein the transition metal is chromium and the post transition metal is selected from Group 13 of the Periodic Table.

10. The system of claim 1, wherein the electrolyte solution has an acidic pH.

11. A method of forming oxygenated products comprising:

providing a system as claimed in any preceding claim; and
electrocatalytically reducing the CO_2 to the oxygenated organic products, wherein the oxygenated organic products comprise two or more carbon atoms and/or two or more oxygen atoms.

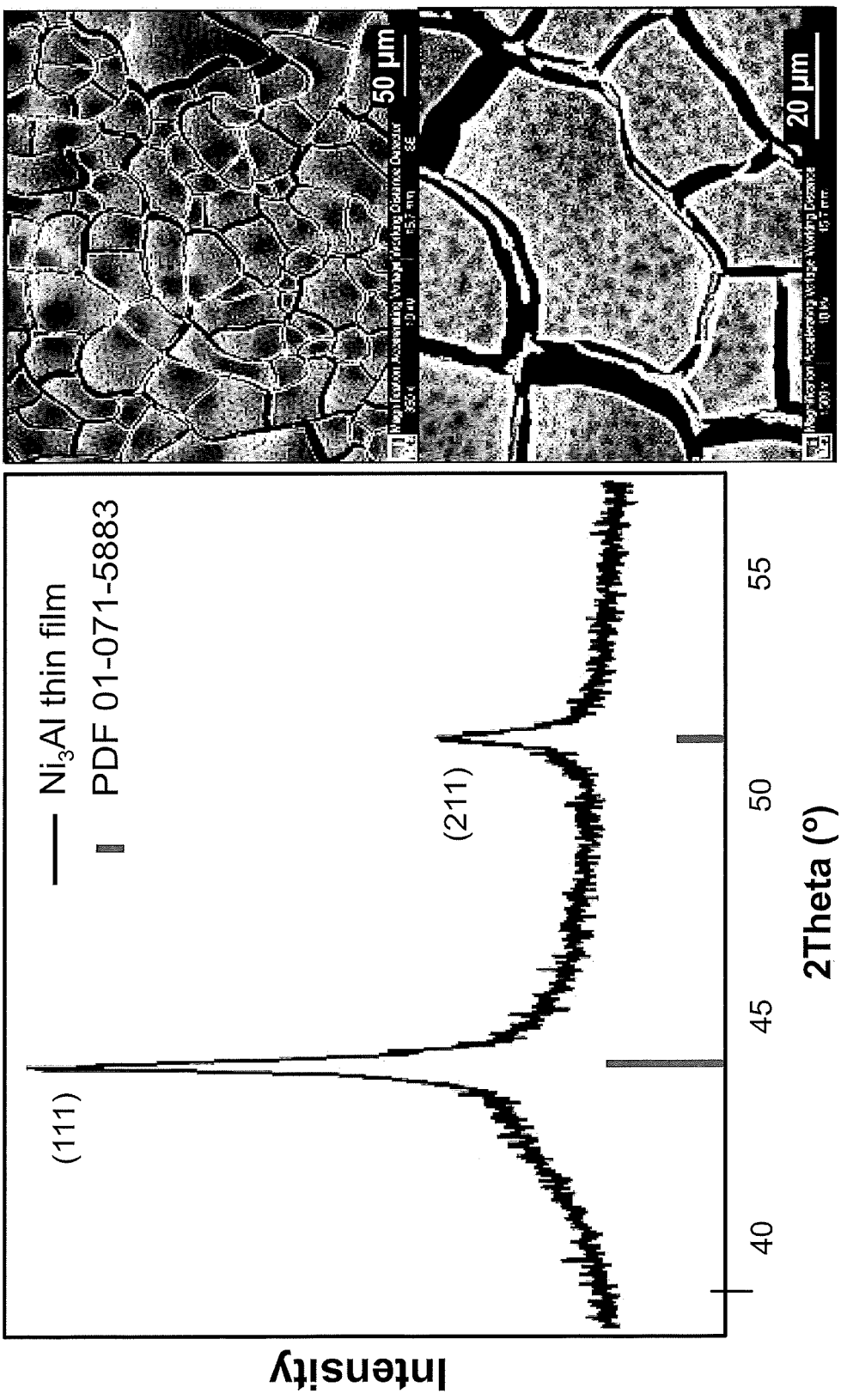
50 µm
20 µm
Ni3Al thin film
PDF 01-071-5883
(111)
(211)
Intensity
40
45
50
55
2Theta (°)

FIG. 1

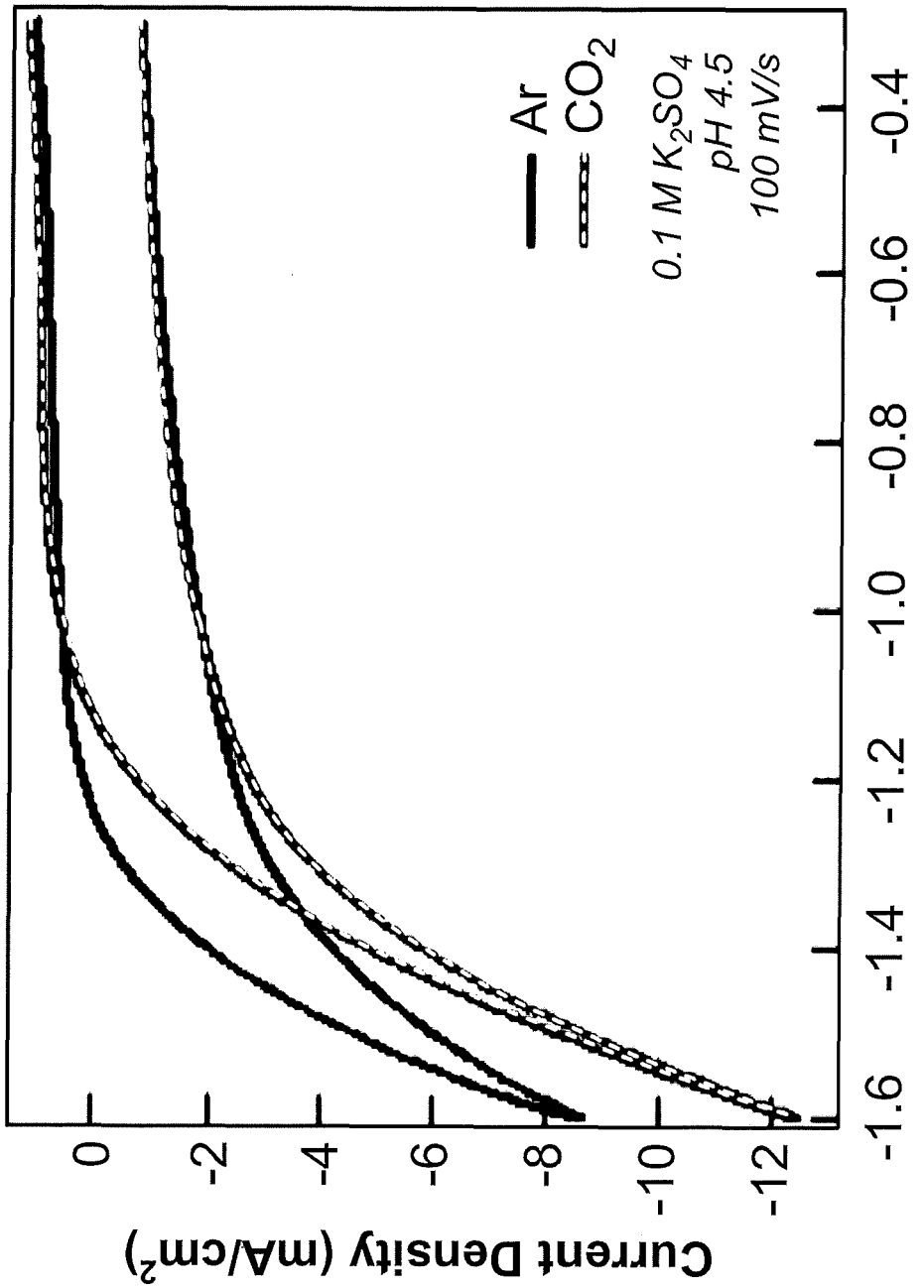
Current Density (mA/cm²)
0
-2
-4
-6
-8
-10
-12
-1.6
-1.4
-1.2
-1.0
-0.8
-0.6
-0.4
Potential (V vs. Ag/AgCl)
Ar
CO2
0.1 M K2SO4
pH 4.5
100 mV/s

FIG. 2A

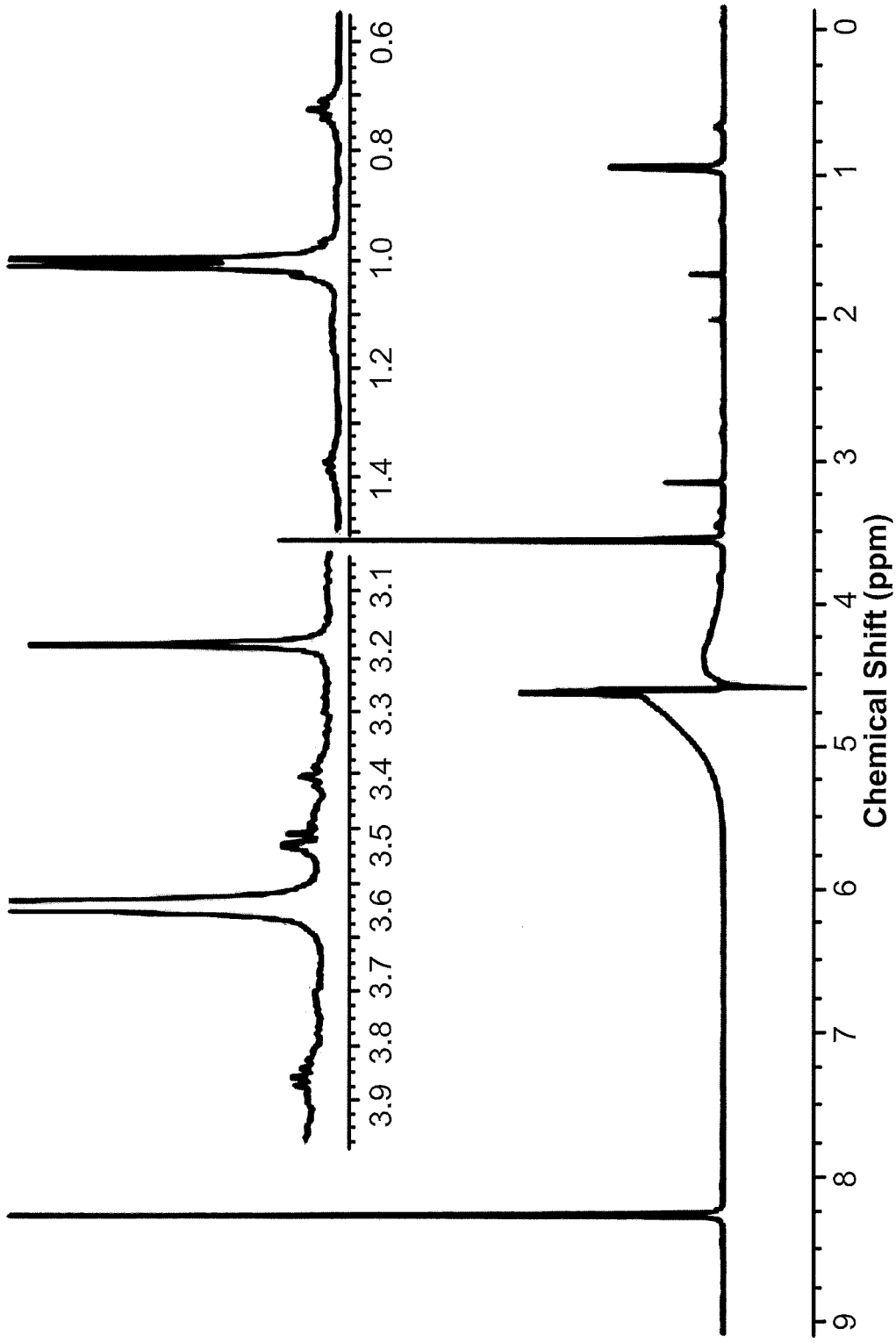
3.9
3.8
3.7
3.6
3.5
3.4
3.3
3.2
3.1
1.4
1.2
1.0
0.8
0.6
9
8
7
6
5
4
3
2
1
0
Chemical Shift (ppm)

FIG. 2B

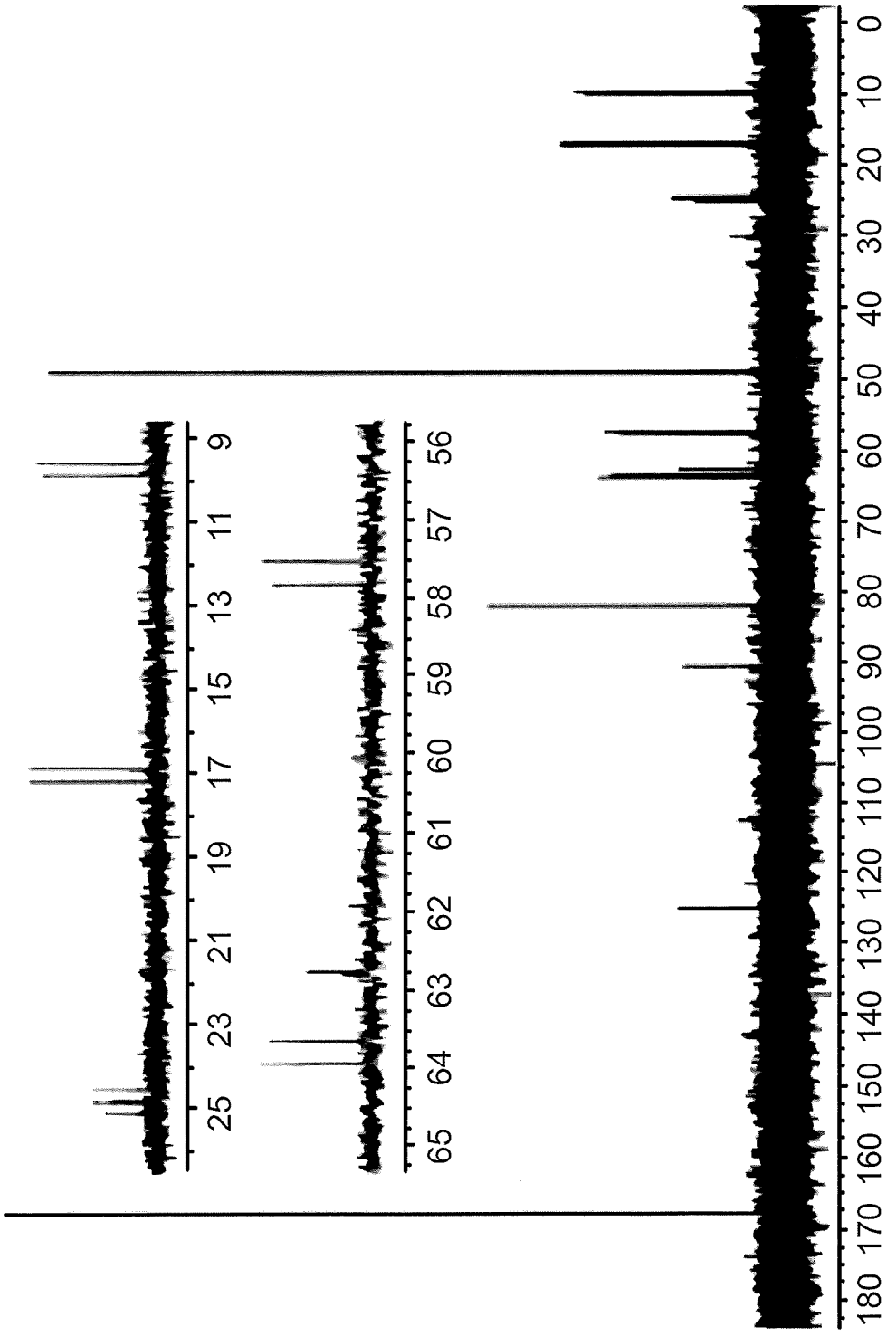
25 23 21 19 17 15 13 11 9
65 64 63 62 61 60 59 58 57 56
180 170 160 150 140 130 120 110 100 90 80 70 60 50 40 30 20 10 0
Chemical Shift (ppm)

FIG. 2C

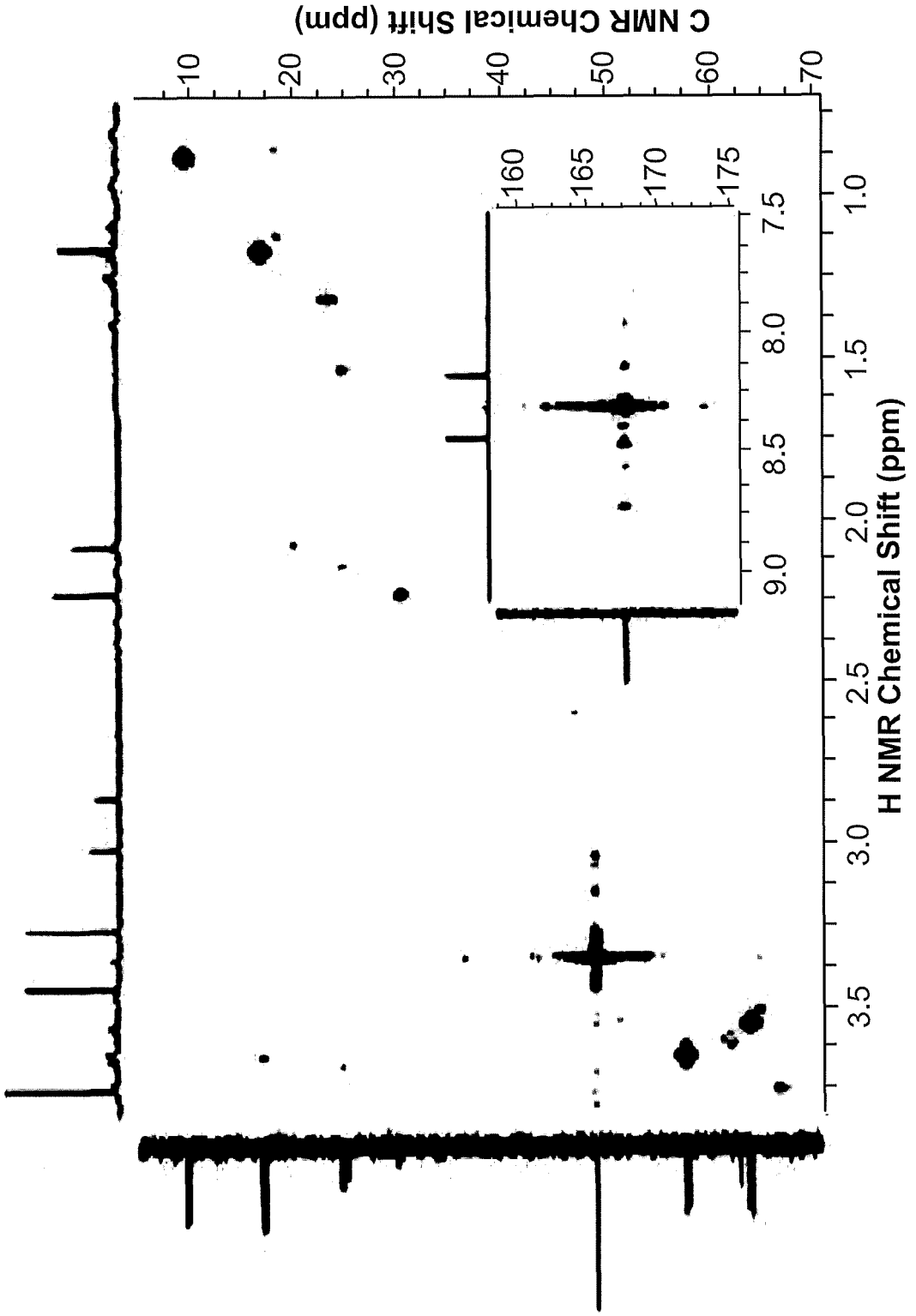
C NMR Chemical Shift (ppm)
10
20
30
40
50
60
70
160
165
170
175
7.5
8.0
8.5
9.0
1.0
1.5
2.0
2.5
3.0
3.5
H NMR Chemical Shift (ppm)

FIG. 2D

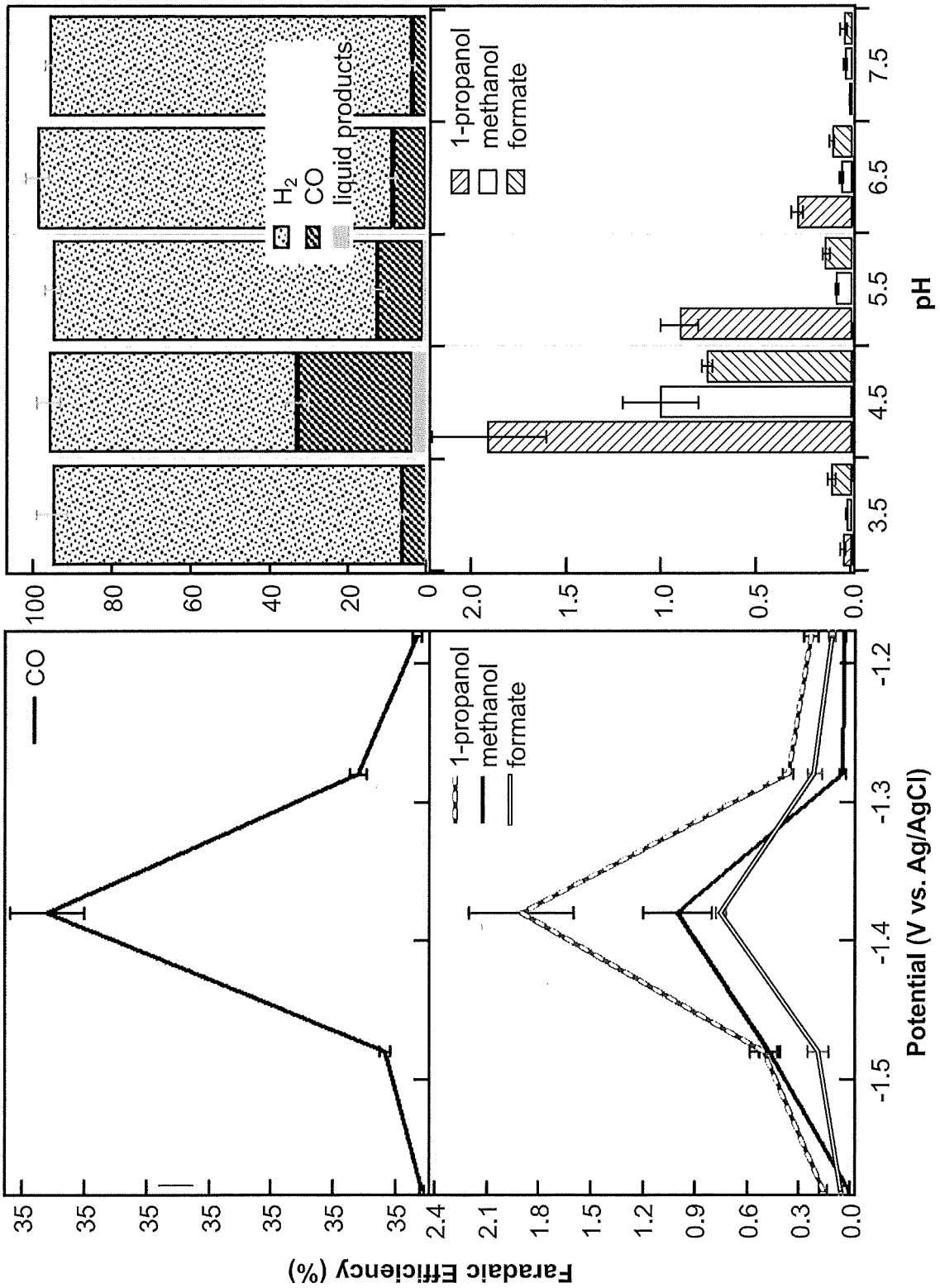
CO
1-propanol
methanol
formate
Faradaic Efficiency (%)
Potential (V vs. Ag/AgCl)
H2
CO
liquid products
pH

FIG. 3A

FIG. 3B

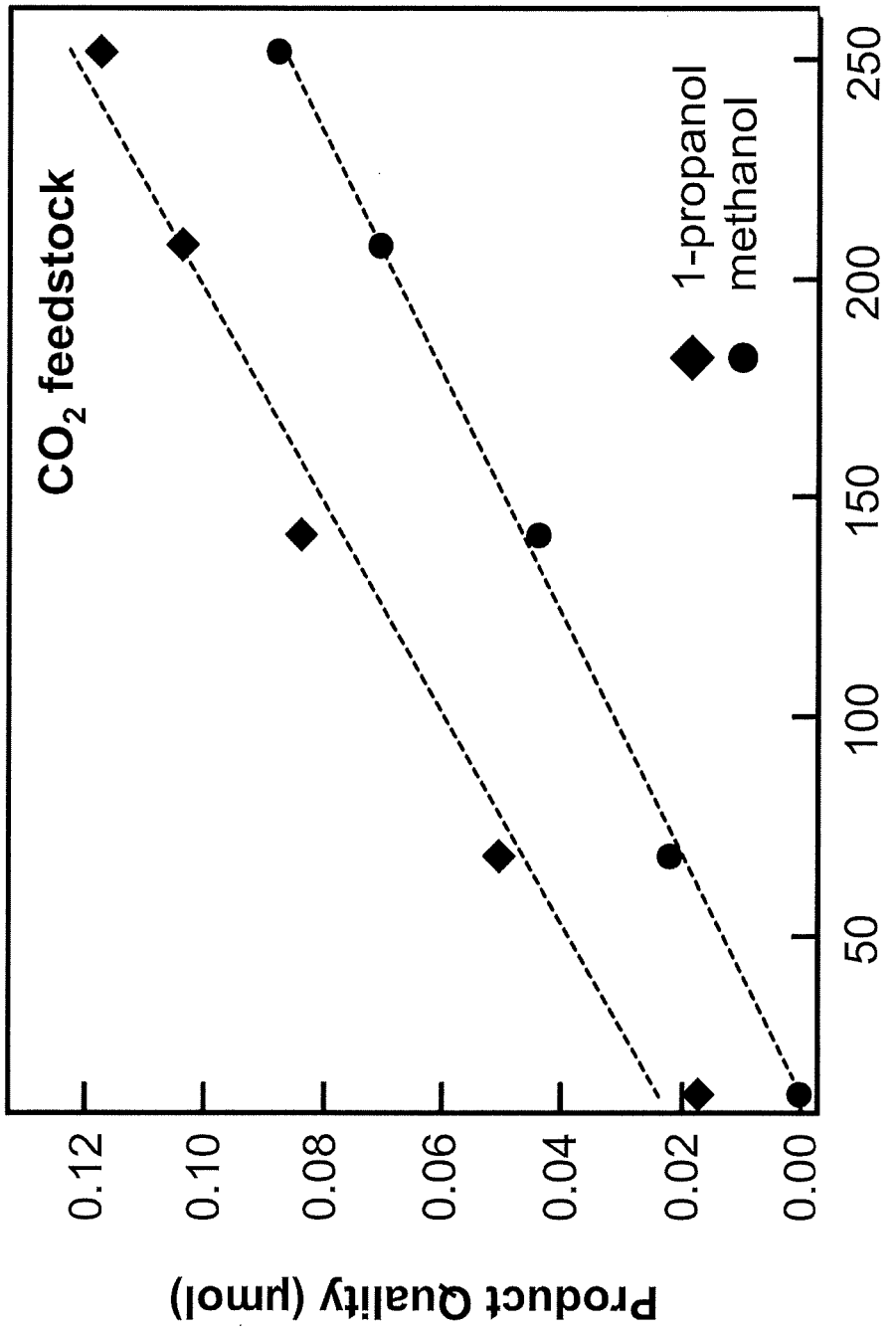
CO_2 feedstock
1-propanol
methanol
Product Quality (μmol)
0.12
0.10
0.08
0.06
0.04
0.02
0.00
50
100
150
200
250
Charge (C)

FIG. 4A

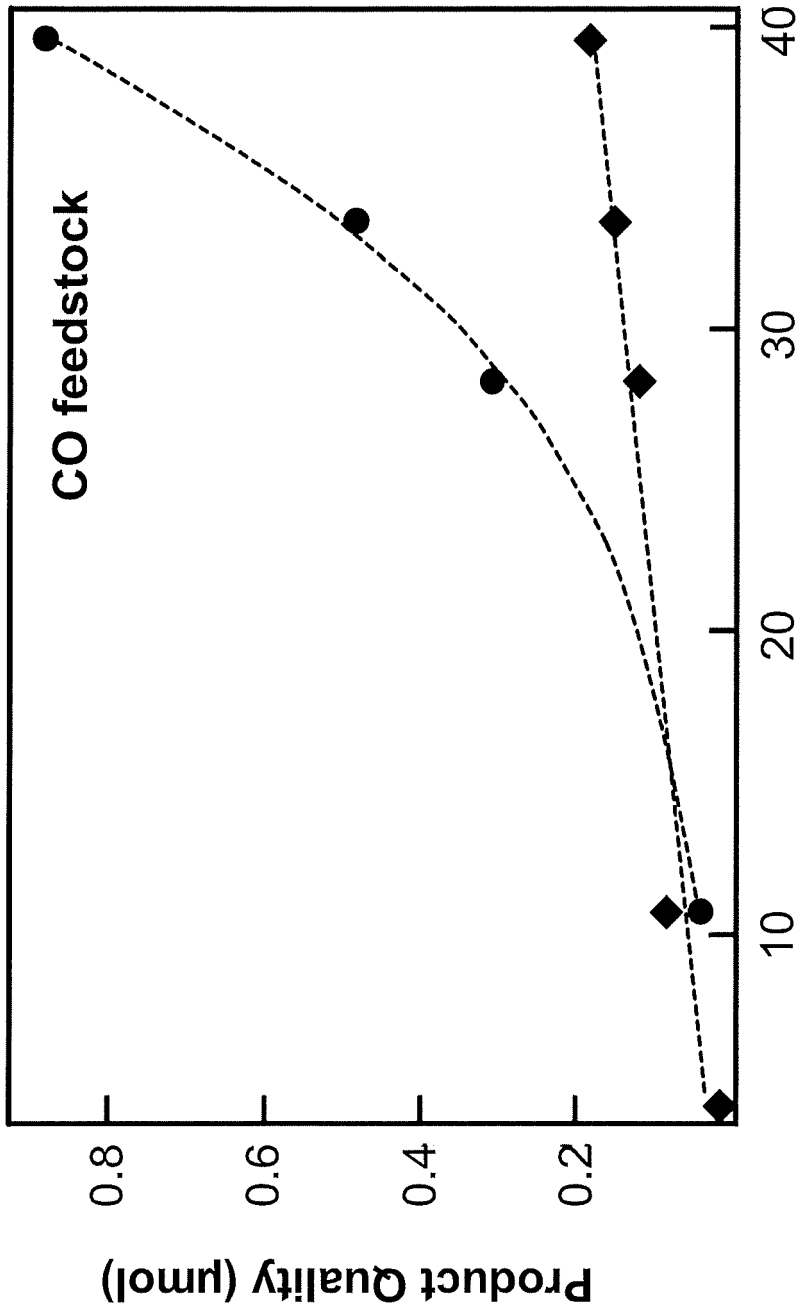
CO feedstock
Product Quality (µmol)
0.8
0.6
0.4
0.2
10
20
30
40
Charge (C)

FIG. 4B

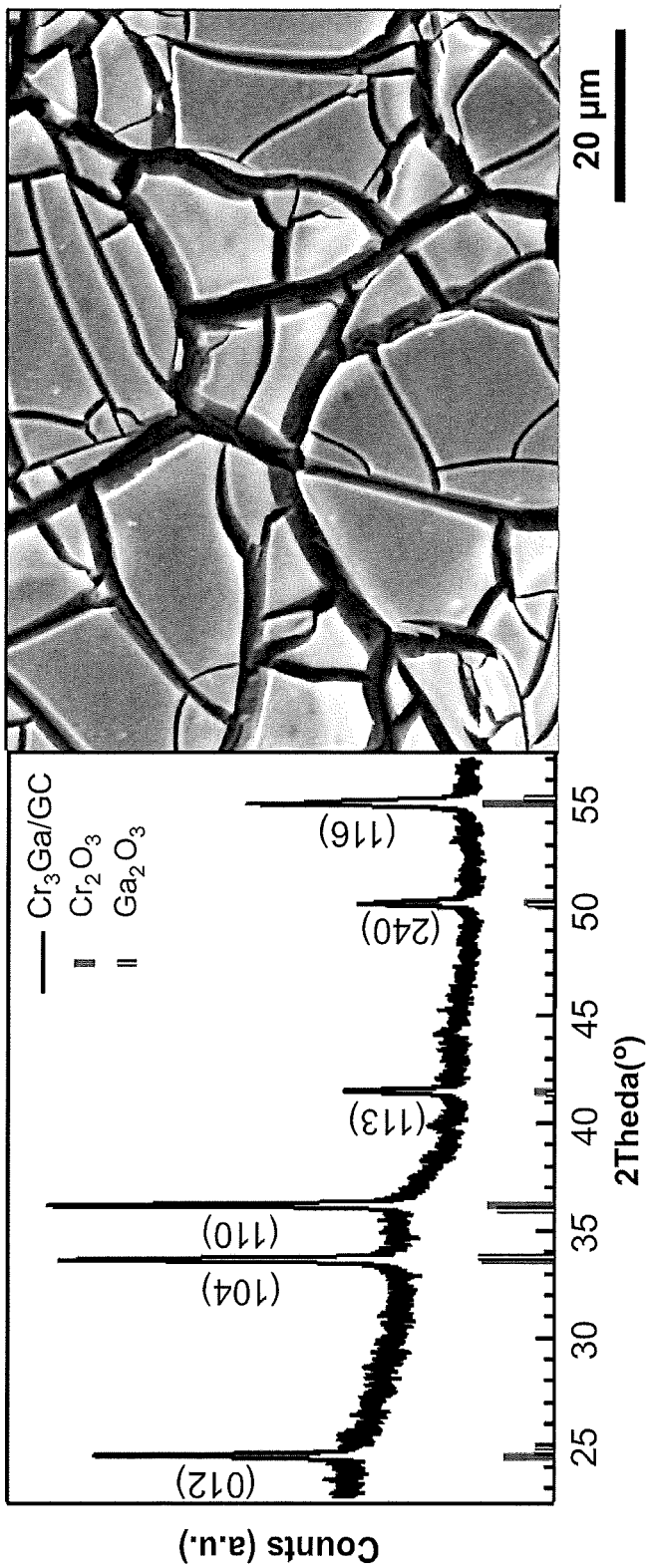
20 μm
Cr3Ga/GC
Cr2O3
Ga2O3
(012)
(104)
(110)
(113)
(240)
(116)
25
30
35
40
45
50
55
2Theda(°)
Counts (a.u.)

FIG. 5A

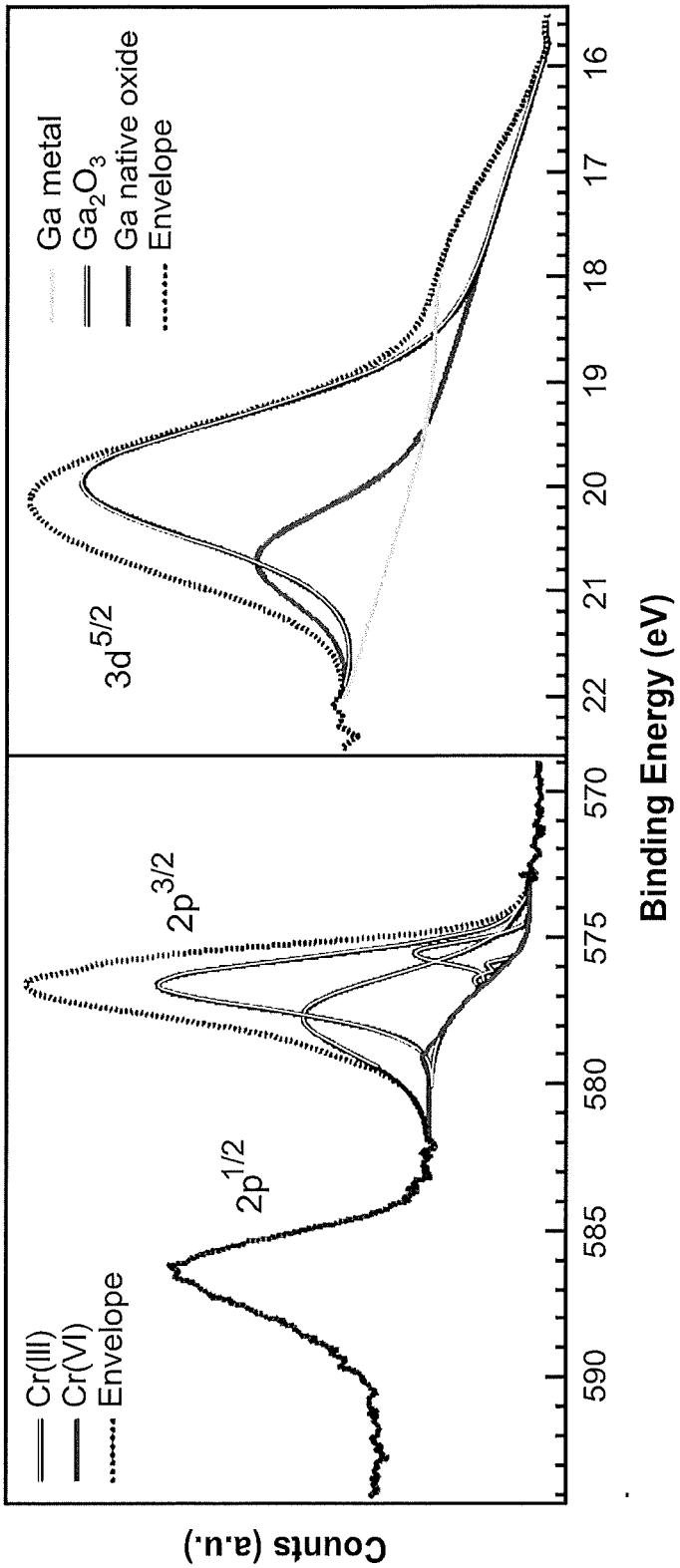
Ga metal
Ga_2O_3
Ga native oxide
Envelope
$3d^{5/2}$
Cr(III)
Cr(VI)
Envelope
$2p^{1/2}$
$2p^{3/2}$
590
585
580
575
570
22
21
20
19
18
17
16
Binding Energy (eV)
Counts (a.u.)

FIG. 5B

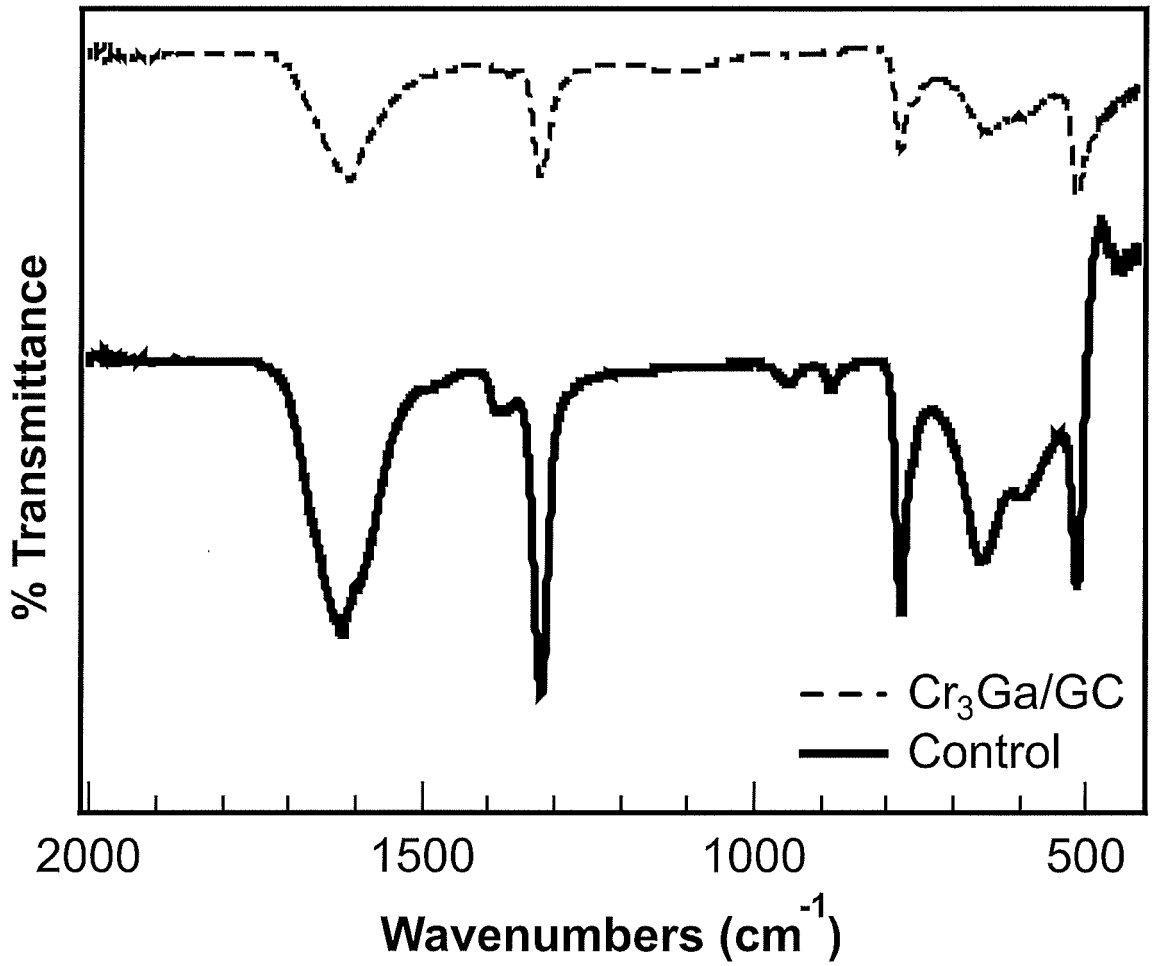
% Transmittance
2000
1500
1000
500
Wavenumbers (cm-1)
Cr3Ga/GC
Control

FIG. 6

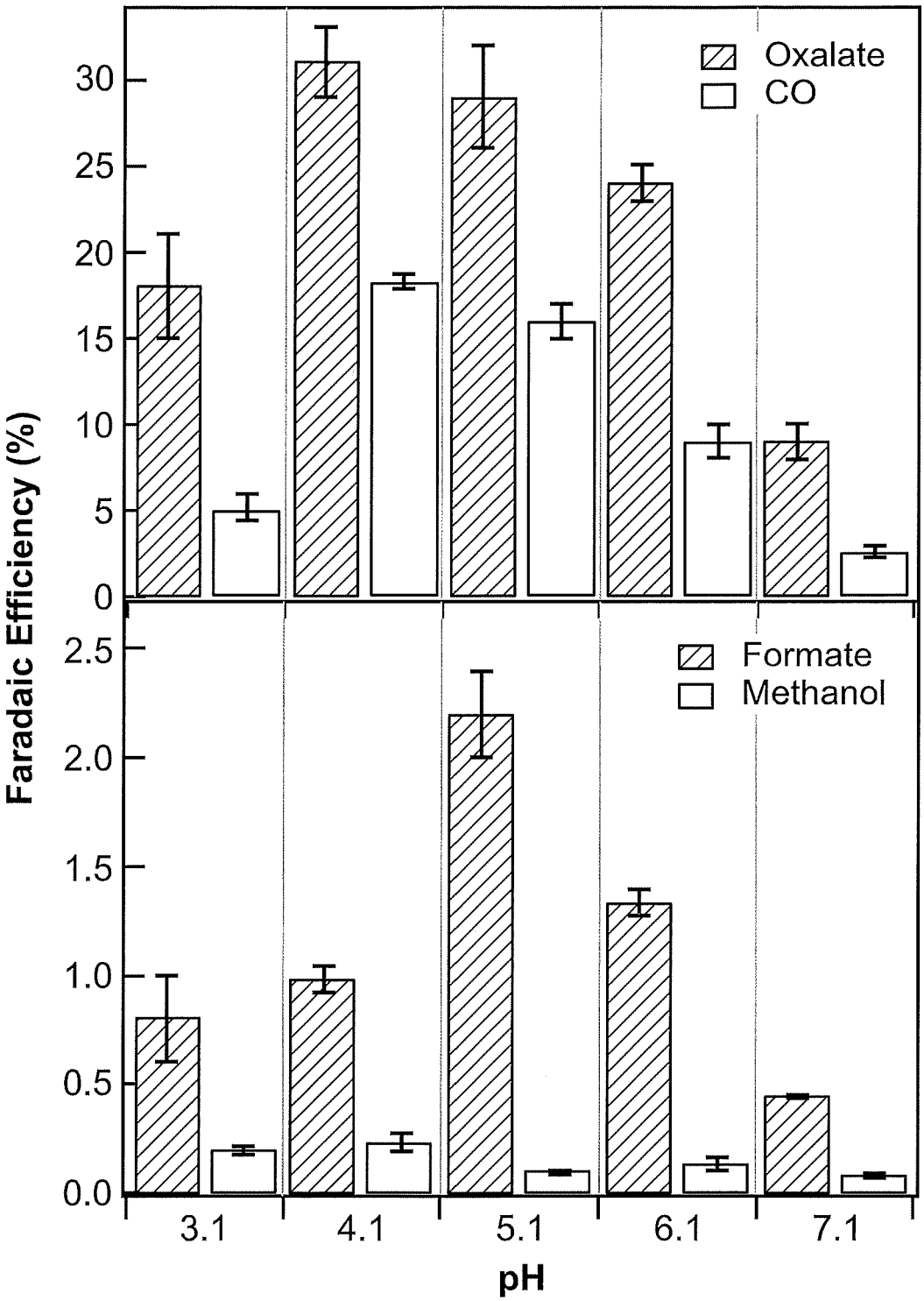
Faradaic Efficiency (%)
30
25
20
15
10
5
0
Oxalate
CO
2.5
2.0
1.5
1.0
0.5
0.0
Formate
Methanol
3.1
4.1
5.1
6.1
7.1
pH

FIG. 7

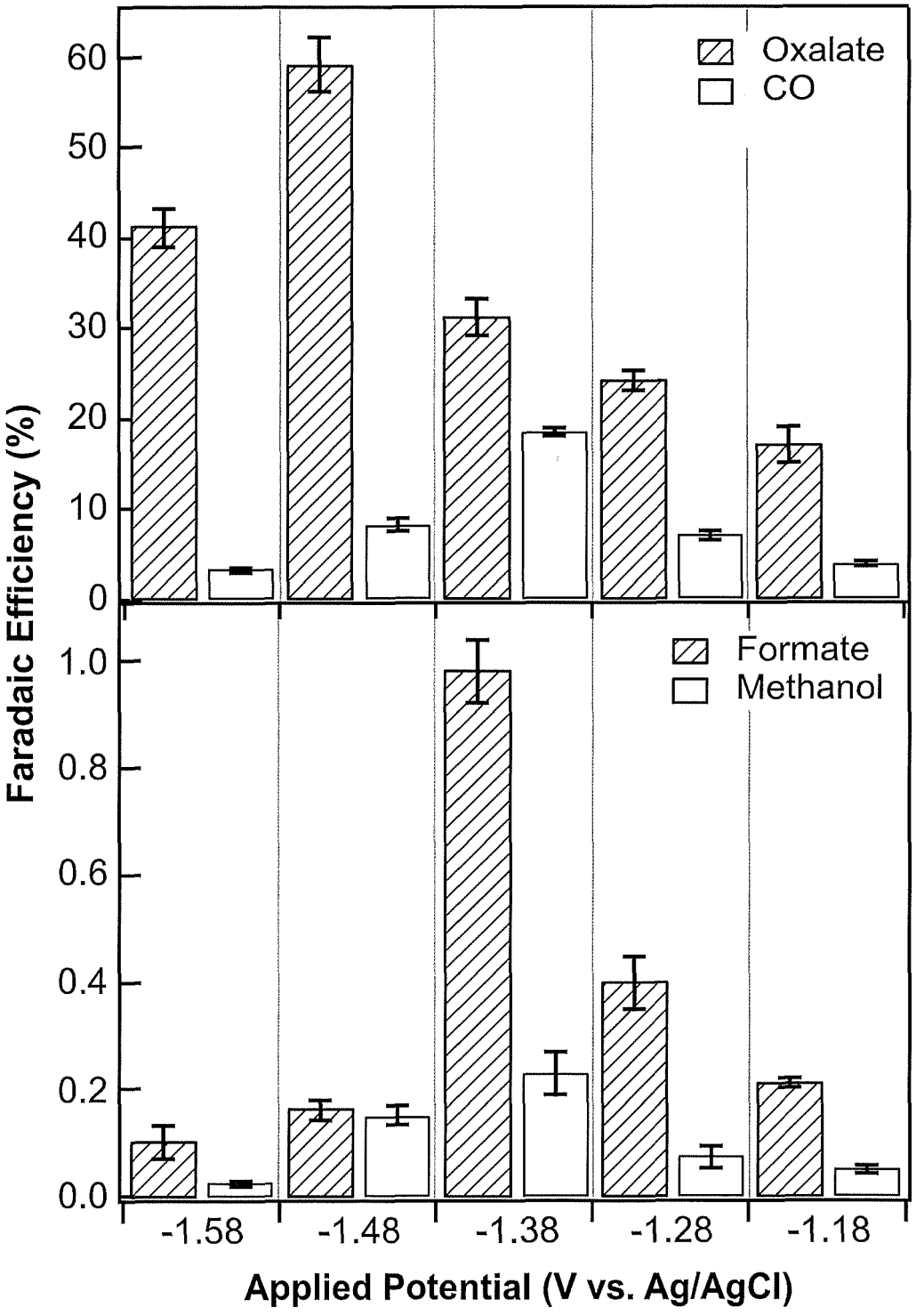
Oxalate
CO
Formate
Methanol
Faradaic Efficiency (%)
60
50
40
30
20
10
0
1.0
0.8
0.6
0.4
0.2
0.0
-1.58
-1.48
-1.38
-1.28
-1.18
Applied Potential (V vs. Ag/AgCl)

FIG. 8

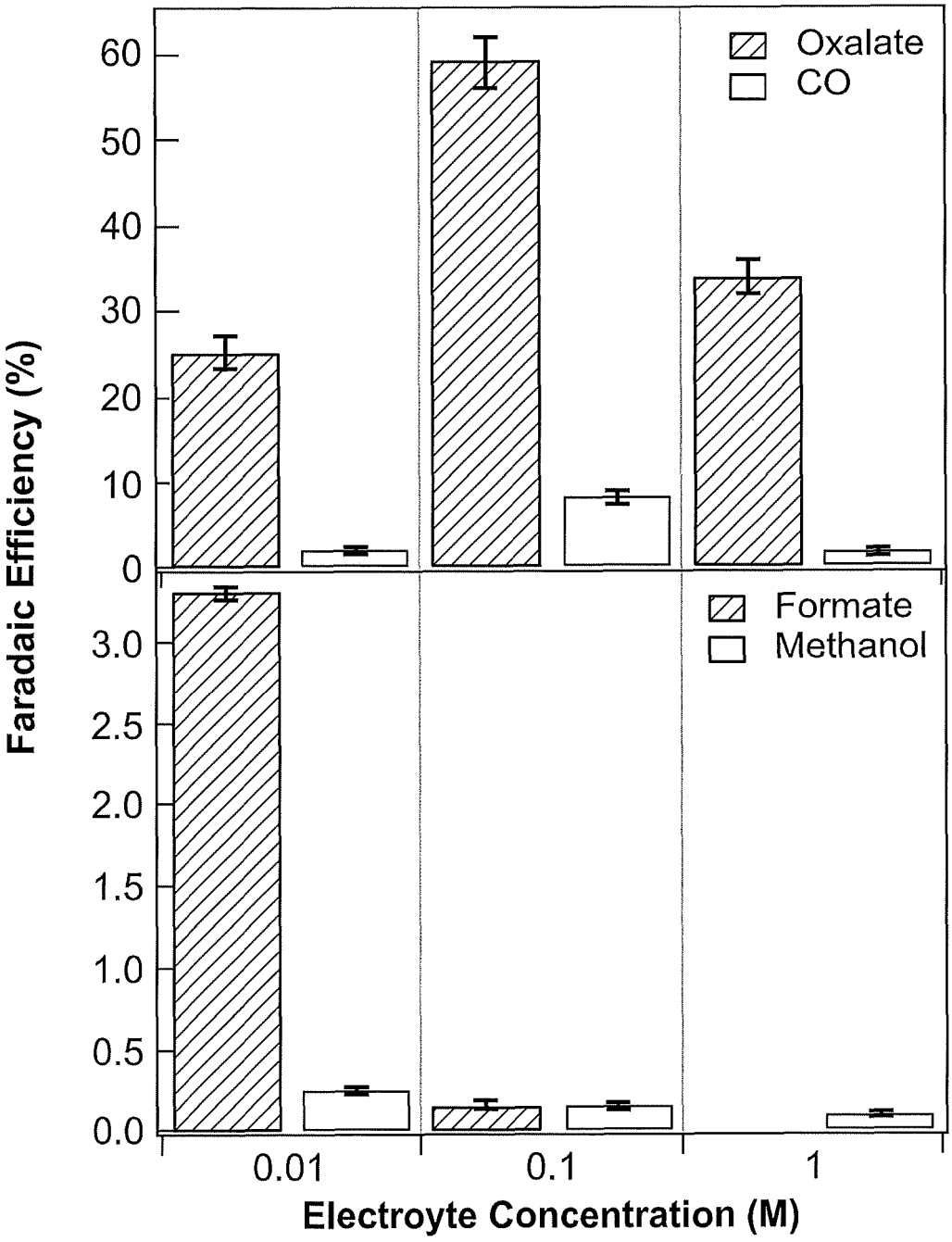
Oxalate
CO
Formate
Methanol
Faradaic Efficiency (%)
60
50
40
30
20
10
0
3.0
2.5
2.0
1.5
1.0
0.5
0.0
0.01
0.1
1
Electroyte Concentration (M)

FIG. 9

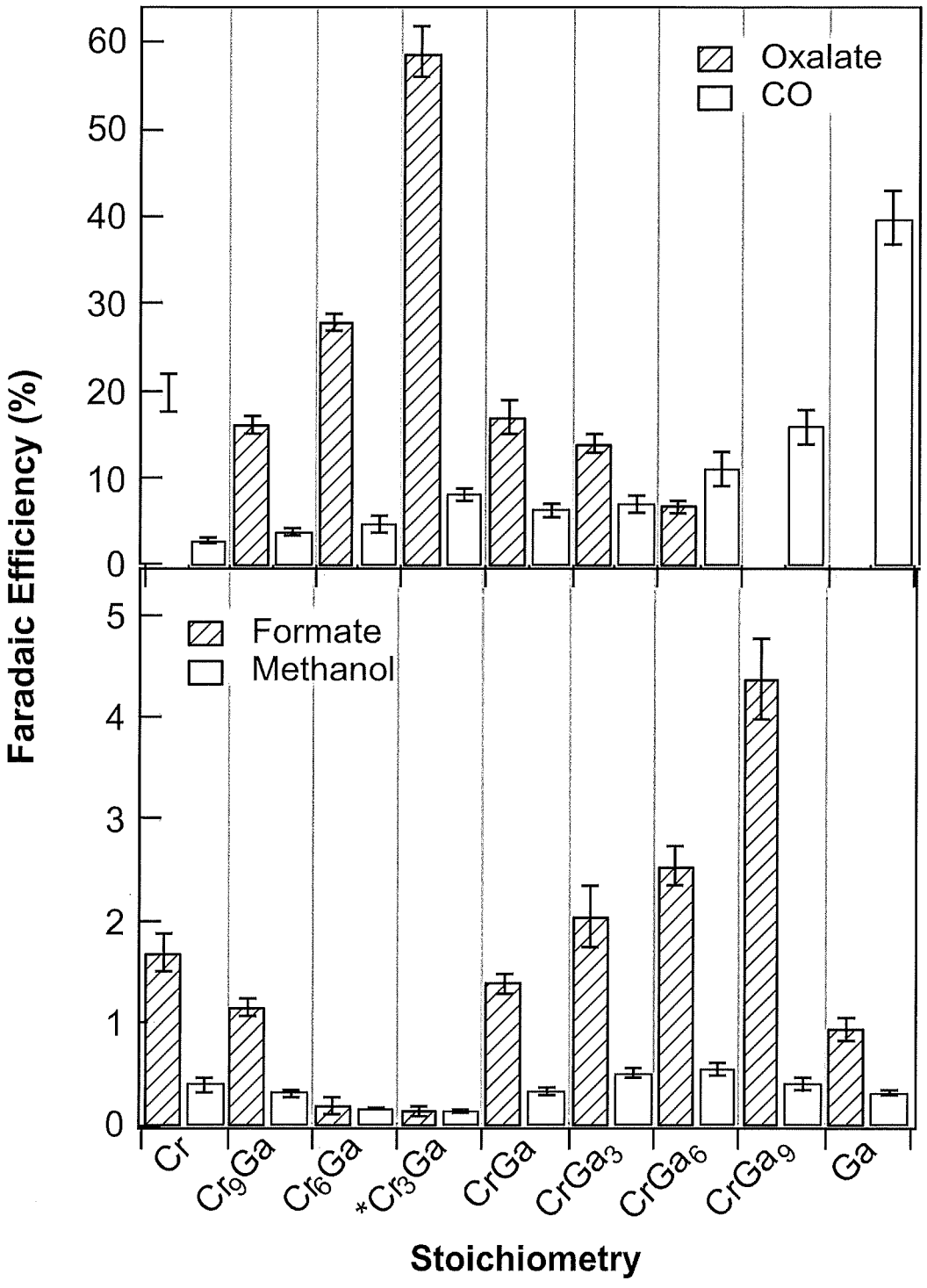
Faradaic Efficiency (%)
Oxalate
CO
Formate
Methanol
Cr
Cr9Ga
Cr6Ga
*Cr3Ga
CrGa
CrGa3
CrGa6
CrGa9
Ga
Stoichiometry

FIG. 10

REFERENCES CITED IN THE DESCRIPTION

This list of references cited by the applicant is for the reader's convenience only. It does not form part of the European patent document. Even though great care has been taken in compiling the references, errors or omissions cannot be excluded and the EPO disclaims all liability in this regard.

Patent documents cited in the description

- US 62555503 **[0002]**
- US 62464816 **[0002]**

Non-patent literature cited in the description

- **TORELLI et al.** *ACS Catal.,* 2016, vol. 6, 2100-2104 **[0023]**
- **TORELLI et al.** Nickel-gallium-catalyzed electrochemical reduction of CO2 to highly reduced products at low overpotentials. *ACS Catal.,* 2016, vol. 6, 2100-2104 **[0038]**